TAMPEREEN TEKNILLINEN YLIOPISTO
TAMPERE UNIVERSITY OF TECHNOLOGY

JARKKO LAAJA

DRONE ENHANCED CONNECTIVITY TO CELLULAR NETWORKS IN DISTURBANCE SCENARIOS

Master's thesis

Examiners: Professor Mikko Valkama and D.Sc. (Tech.) Joonas Säe

The examiners and topic of the thesis were approved on 29 August 2018

ABSTRACT

JARKKO LAAJA: Drone Enhanced Connectivity to Cellular Networks in Disturbance Scenarios
Tampere University of Technology
Master of Science Thesis, 57 pages, 10 Appendix pages
November 2018
Master's Degree Programme in Information Technology
Major: Communication Systems and Networks
Examiners: Professor Mikko Valkama and D.Sc. (Tech.) Joonas Säe

Keywords: drone, UAV, cellular networks, LTE, base station, disturbance scenario, distribution network, electrical grid

Power outages caused by intense storms require a vast repair operation to restore power. During these disturbance scenarios, repair workers need a cellular connection in order to fulfill their work assignments. However, the cellular network base stations that provide coverage to the repair area might be effected by the blackout. The reserve batteries on these base stations last only a couple of hours. To solve this lack of cellular connectivity, repair crews have to drive several kilometres searching for a working connection. This delays the repair process a great deal.

This thesis examines using a drone to solve this connectivity problem. Even though there is no working connection at the ground level, a functioning communication link could be achieved above the tree tops, where there is less signal attenuation from trees and hills. With increased altitude, the drone should be able to achieve a line-of-sight connection to farther away base stations that are still in working order. These better signal propagation conditions were the premise of this study. The proposed solution is to attach a cell phone to the drone and share the phone's cellular connection as a Wi-Fi hotspot to the repair crew on the ground.

To analyse the feasibility of such a solution, a measurement campaign was performed in rural areas in the Pirkanmaa region. The phone attached to the drone measured cellular network parameters, such as signal strength and signal quality. The primary objective was to research the effect of altitude on these performance parameters. Additionally, another area of focus was to study the cell phone's connection to distant base stations that are not available at the ground level. For that reason, the drone flew predetermined, autonomous flight routes around the measurement sites at altitudes of 50 m, 100 m, and 150 m. During these flight paths, the phone measured the performance of 2G GSM, 3G UMTS, and 4G LTE networks.

The results indicate that signal strength increases considerably with increased altitude. In the air, the phone has a 20–30 dB stronger received signal power compared to the ground level. However, at the same time, signal quality decreases, as the phone suffers interference from other base stations. Furthermore, this improvement of signal power results in an increase of signal range. The phone was able to connect to base stations tens of kilometres away from the measurement site. This increased signal range means that the repair team is able to get a working cellular connection from the repair site without having to look for a signal. Using a drone as a temporary access point is a viable solution in disturbance scenarios and warrants further research on this topic.

TIIVISTELMÄ

JARKKO LAAJA: Kauko-ohjattavien lennokkien hyödyntäminen matkapuhelinverkkojen kuuluvuusalueiden laajentamiseksi poikkeustilanteissa
Tampereen teknillinen yliopisto
Diplomityö, 57 sivua, 10 liitesivua
Marraskuu 2018
Tietotekniikan diplomi-insinöörin tutkinto-ohjelma
Pääaine: Communication Systems and Networks
Tarkastajat: professori Mikko Valkama ja TkT Joonas Säe

Avainsanat: drone, miehittämätön ilma-alus, matkapuhelinverkko, LTE, tukiasema, häiriötilanne, jakeluverkko, sähköverkko

Rajujen myrskyjen aiheuttamat sähkökatkokset vaativat laajan korjausoperaation sähkönjakelun palauttamiseksi. Näissä suurhäiriötilanteissa korjaustyöntekijät tarvitsevat matkapuhelinyhteyden käyttökeskukseen saadakseen tietoa sähköverkon tilasta. Sähkökatkos voi vaikuttaa myös matkapuhelinverkon tukiasemiin. Näiden tukiasemien varavirtalähteet kestävät vain pari tuntia. Jos korjauspaikalta ei saada yhteyttä käyttökeskukseen, korjaajien täytyy etsiä toimivaa signaalia auton avulla. Tämä aiheuttaa viivästyksiä korjausprosessiin.

Tämä diplomityö tutkii dronen käyttöä tämän ongelman ratkaisemiseksi. Vaikka maanpinnan tasolla ei ole toimivaa matkapuhelinyhteyttä, puiden latvojen yläpuolella, jossa puut ja kukkulat eivät vaikuta signaalin vaimentumiseen, voisi löytyä toimiva yhteys. Korkealla ilmassa dronen pitäisi pystyä saavuttamaan näköyhteys kauempina sijaitseviin tukiasemiin, joihin sähkökatkos ei ole vaikuttanut. Tämän tutkimuksen lähtökohtana olivat nämä ilmassa olevat paremmat signaalin etenemisolosuhteet. Ratkaisuna esitetään kiinnittää matkapuhelin droneen kiinni ja jakaa tämän puhelimen mobiiliyhteys Wi-Fi-hotspotin avulla maantasalla oleville korjaajille.

Tämän ratkaisun käyttökelpoisuuden analysoimiseksi suoritettiin matkapuhelinverkon mittauksia haja-asutusalueilla Pirkanmaan seudulla. Droneen kiinnitetty puhelin mittasi matkapuhelinverkon parametrejä, kuten signaalin voimakkuutta ja signaalin laatua. Ensisijaisena tavoitteena oli selvittää korkeuden vaikutus näihin suorituskykyparametreihin. Toinen painopiste oli tutkia matkapuhelinyhteyttä kaukaisiin tukiasemiin, jotka eivät ole saatavilla maanpinnalla. Tästä syystä drone lensi ennalta määrättyjä, autonomisia lentoreittejä 50 m, 100 m ja 150 m korkeuksissa. Näiden lentoreittien aikana puhelin mittasi 2G GSM-, 3G UMTS- ja 4G LTE -verkkojen suorituskykyä.

Tulokset osoittavat, että signaalin voimakkuus kasvaa huomattavasti dronen korkeuden noustessa. Ilmassa olevassa puhelimessa on 20–30 dB vahvempi vastaanottoteho verrattuna maanpinnan tasoon. Samanaikaisesti signaalin laatu heikkenee, koska puhelin kärsii muista tukiasemista aiheutuvasta häiriöistä. Tämä signaalitehon parannus johtaa signaalin kantaman nousuun. Puhelin pystyi muodostamaan yhteyksiä tukiasemille, jotka olivat kymmenien kilometrien päässä mittauspaikalta. Tämä lisääntynyt signaalikantama tarkoittaa, että korjausryhmä saa toimivan matkapuhelinyhteyden korjauspaikalta ilman, että signaalia tarvitsee etsiä auton avulla. Dronen käyttö matkapuhelinverkkojen kuuluvuusalueiden laajentamiseksi poikkeustilanteissa on lupaava ratkaisu ja edellyttää lisätutkimuksia.

PREFACE

The research for this thesis was performed at the Laboratory of Electronics and Communication Engineering at Tampere University of Technology. I would like to thank my supervisor Joonas Säe for the guidance, input, and invaluable feedback. Joonas played a vital role in the successful completion of this project. I would also like to express my gratitude towards Mikko Valkama, who, along with Joonas Säe, examined my thesis and enabled an inspiring atmosphere and a great working environment at the laboratory.

The idea for this thesis originated from Heikki Paananen from Elenia Oy, who commissioned this thesis. He also acted as the company contact person. Heikki gave excellent advice, helped me set up the interviews, and was a pleasure to work with.

I would also like to thank Toni Levanen for the advice and input, Julius Tamminen for helping with the measurements, Richard Wirén for the drone advice, my work roommates Juha Yli-Kaakinen and Alaa Loulou for the guidance and laughter, and Marcelo Fabián Trujillo Fierro for providing peer support for thesis writing.

Finally, I would like to thank my family for the love and support.

In Tampere, Finland, on 24 October 2018

Jarkko Laaja

CONTENTS

LIST OF FIGURES

LIST OF TABLES

LIST OF ABBREVIATIONS AND SYMBOLS

3D	Three dimensional
3GPP	3rd Generation Partnership Project
AP	Access point
BA	BCCH allocation
BER	Bit error rate
BS	Base station
BSIC	Base station identity code
BTS	Base transceiver station
BVLOS	Beyond-visual-line-of-sight
C2	Command and control
CID	Cell ID
CPICH	Common pilot channel
CSV	Comma separated value
D2B	Drone-to-base station
DSO	Distribution system operator
E-UTRA	Evolved UMTS terrestrial radio access
EIRP	Effective isotropic radiated power
EURO-COST	The European cooperative for scientific and technical research
FDD	Frequency-division duplexing
FICORA	Finnish Communications Regulatory Authority
FSPL	Free space path loss
GPS	Global positioning system
GSM	Global System for Mobile Communications
IEEE	Institute of Electrical and Electronics Engineers
IMU	Inertial measurement unit
KML	Keyhole markup language
KML	Keyhole markup language
KPI	Key performance indicator
LCID	Long cell ID
LOS	Line-of-sight
LTE	Long-term evolution
MAT	Matlab file format
MNO	Mobile network operator
MS	Mobile station
NB	Node B
NLOS	Non-line-of-sight
NMF	Nemo file format
PCI	Physical cell identity
PSC	Primary scrambling code
RC	Remote controller
RNC	Radio network controller
RPA	Remotely piloted aircraft
RSCP	received signal code power
RSRP	Reference signal received power
RSSI	Received signal strength indicator
RTH	Return to home
RX	Receiver

SHO	Soft handover
SINR	Signal-to-interference-plus-noise ratio
TUT	Tampere University of Technology
TX	Transmitter
Trafi	Finnish Transport Safety Agency
UAV	Unmanned aerial vehicle
UE	User equipment
UMTS	Universal mobile telecommunications system
UMa	Urban macro
UMi	Urban micro
VLOS	Visual-line-of-sight
VoWi-Fi	Voice over Wi-Fi
Wi-Fi	Radio technology for local wireless networks
eNB	Evolved node B

d_{km}	2D distance to the base station
d_{3D}	3D distance to the base station
E_c/N_0	Received energy per chip divided by the power density in the band
$f_{\text{c-MHz}}$	Carrier frequency
G_{antenna}	Antenna gain
h_{UE}	User equipment antenna height
h_{BS}	Base station antenna height
L_{cable}	Cable loss
N	LTE resource block
P_{TX}	Transmitted power

1. INTRODUCTION

In recent years, unmanned aerial vehicles (UAVs), that is, drones, have been used for a wide range of commercial and civil applications. Aerial photography, search and rescue, gas or oil pipeline inspections, agricultural surveys, infrastructure maintenance, and various law enforcement and military functions have seen an increase in the use of drones. [29, 41] As drones are becoming a common tool for many industries, it is important to focus on their connectivity aspects.

Recently, a lot of research [1, 4–6, 8, 20, 32, 38, 39, 43, 46, 47, 54, 56, 59–61] has been focusing on using long-term evolution (LTE) networks to provide a reliable link for drone command and control (C2) functions. These have been studied in beyond-visual-line-of-sight (BVLOS) situations, where the drone is controlled by the cellular network. Additionally, drones can be used as ad-hoc base stations in disaster scenarios [11, 12]. Furthermore, [27] has researched a mass deployment of a fleet of drones to provide connectivity to several people. However, using drones to extend the coverage of cellular networks [7, 13] has not seen an equal amount of effort.

This thesis examines using a drone as an access point (AP) to provide cellular connectivity to a single user in electrical grid disturbance scenarios. The purpose of this thesis is to research drones as a way to expand the coverage of cellular networks in situations where normal cell coverage is temporarily unavailable or out of reach. The goal of this thesis is to find a solution to cellular network connectivity issues during disturbance scenarios. This solution entails attaching a mobile phone to the drone, which provides cellular connectivity to the ground with a Wi-Fi hotspot. Higher up in the air, the drone would have connectivity to base stations that are not available at the ground level due to better signal propagation conditions. To examine the validity of such a solution, a measurement campaign was carried out at five locations in the Pirkanmaa region. The main research questions were to determine, how does signal strength increase in the air compared to the ground level and what effect does the increased height have on signal quality, signal range, and base station connectivity. The scope of this thesis is to determine the feasibility of such a connection for electrical grid repair scenarios and to study the propagation characteristics of cellular networks in various altitudes.

2. MOTIVATION

Elenia Oy, a Finnish distribution system operator (DSO), commissioned this thesis. Elenia operates in several local districts in Southern and Central Finland [16].

2.1 Problem statement

Extreme weather conditions, such as storms, can cause electrical grid disturbance scenarios. A disturbance scenario means a power outage in the electrical grid caused by trees falling on an overhead power line for example. [53] This power outage will affect nearby cellular network base stations as well. These base stations have reserve batteries that last only a few hours [23]. Once the base stations lose power, the immediate area can be out of cellular network connectivity. During these blackouts, DSOs mobilize a great number of repair workers and equipment to restore power distribution.

However, the repair workers who have been dispatched to restore power require a voice or a data connection to a control center that is coordinating the repairs. The repair team has to report the status of the repairs, get work orders for the next task, and retrieve information about the status of the electrical grid using mobile networks. Currently, in order to gain connectivity, they have to drive several kilometres to an area that has cellular coverage. This travelling causes significant delays to the electrical grid repairs. Figure 2.1 illustrates the problem of having to drive several kilometres from the repair site to gain connectivity to a cellular network. [36, 51, 52]

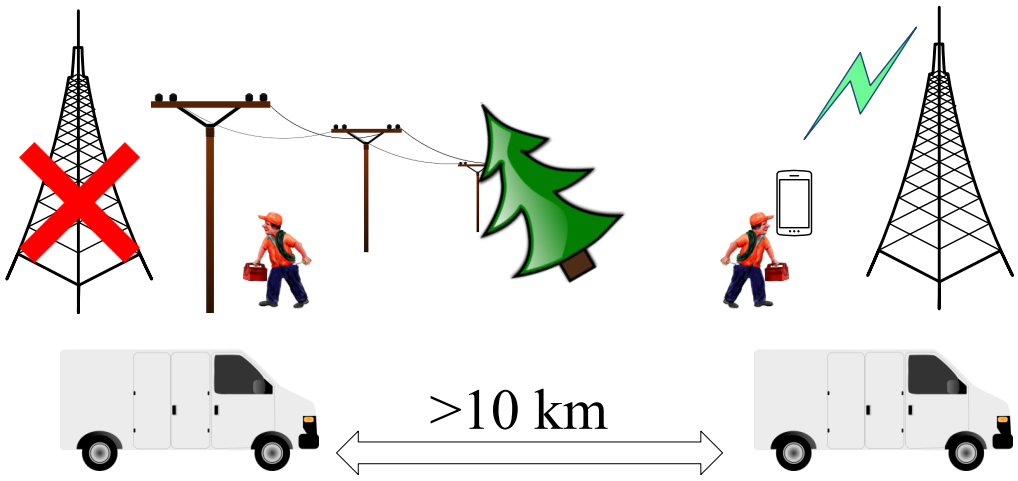

Figure 2.1. *Problem: searching for a working cellular signal by car during a disturbance scenario.*

As a solution to this problem, this thesis examines using a drone to gain cellular connectivity at the repair site. Even though there is no cellular coverage at ground level, higher up, above the tree top level, there might be coverage from far away base stations that have not been effected by the power outage. The hovering drone would be able to share this working cellular connection to the repair crew with a Wi-Fi access point, for example. The repair workers would have access to a voice or data connection without having to look for a signal using a car. This would expedite the repair operation significantly. Figure 2.2 depicts the solution of using a drone as a temporary access point.

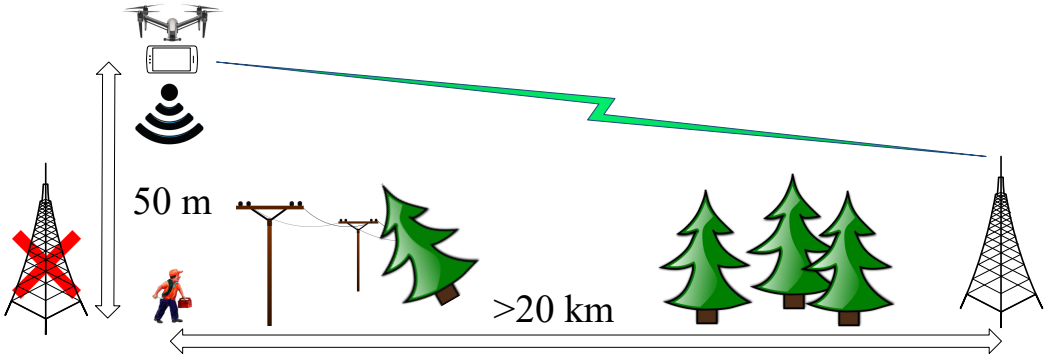

Figure 2.2. *Solution: using a drone to connect to a distant base station to achieve cellular connectivity.*

2.2 Drone usage in electrical grid repair work

To gain insight and to determine the current status of drone usage in electrical grid repair work, three interviews were conducted. The interviewees were potential end users of the proposed solution or managers in charge of drone utilisation. The interview script can be found in appendix C.

At the moment, drones are used for inspecting aerial components, assessing the damage to overhead power lines, or locating the repair site by using the drone's camera. A drone can find the repair site relatively quickly compared to the traditional methods of on foot, by car, or with a quad bike. The advantage is significant especially in hard-to-reach places, such as in island locations.

Every interviewee remembers a situation, where cellular connectivity was not available at the repair site and a car was used to search for a working cellular signal. So far, there has not been any attempts to solve this problem.

At present, the use of drones is at a pilot stage. Only a handful of repair crews use drones in their maintenance tasks. However, there are some plans in place to expand the current drone operations. The main obstacles against a wide spread use of drones are the cost-effectiveness and legislation against BVLOS flights. [36, 51, 52]

3. THEORY AND CONCEPTS

The premise of this thesis is that the propagation conditions are more favourable above the tree tops compared to the ground level. A line-of-sight (LOS) propagation between a drone and a base station would offer less attenuation from trees, buildings, and hills. Furthermore, a drone should be able to connect to base stations that are further than a mobile phone on the ground level is able to. However, modelling this propagation with existing path loss models might not be accurate because these models are only valid in situations, where the base station (BS) height is much higher than the user equipment (UE) height. This chapter discusses signal propagation characteristics, both existing and drone-to-base station (D2B) specific path loss models, key performance indicators for cellular networks, and concepts related to this project.

3.1 Drone connectivity characteristics

Cellular networks are not tailored for aerial coverage. In order to reduce interference to other cells and confine the coverage area, base station antennas are often downtilted [47]. Additionally, since the drone altitude can often exceed the base station antenna height, drones might not fall under the main beam of the base station. Figure 3.1 illustrates how the side lobe of a base station antenna is serving the drone. Both the main lobe and these side lobes can have null zones, which means that the closest base station might not provide the strongest signal to the drone. However, the more favourable propagation conditions in the air might offset the reductions in antenna gain. Furthermore, because of a large line-of-sight propagation probability, a drone suffers interference from more neighboring cells compared to a ground based UE. This interference can result in a poor downlink signal-to-interference-plus-noise ratio (SINR) compared to terrestrial UEs. The drone also has a potential to cause interference to other UEs in the uplink. These differences in coverage and interference characteristics between terrestrial and aerial UEs have an effect on drone based communications. Existing path loss models, power control mechanisms, and handover procedures, for example, might not be valid for aerial UEs. [1, 39]

3.2 Line-of-sight probability

A line-of-sight radio link has no obstacles between the transmitter and receiver. That means that the signal propagates over the air without any hindrance. [39] According to [1], for rural macro (RMa) areas, the LOS probability is 100%, when the aerial UE height is between 40 m and 300 m. For urban macro (UMa) areas, the applicable UE height range is between 100 m and 300 m to achieve a 100% line-of-sight probability. However, these results have assumed antenna heights of 25 m for urban macro, and 35 m for rural macro.

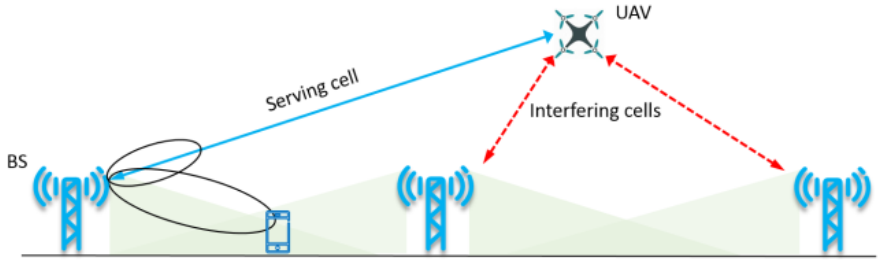

Figure 3.1. *Drone connectivity characteristics. [39] (© 2018 IEEE)*

The measurement campaign for this thesis was conducted in rural macro areas with base station antennas mounted to masts, with antenna heights ranging from 50 m to 70 m. The LOS probability also depends on the distance between the UE and the base station. As a result, it is highly likely that most of the measurements were performed in LOS conditions.

3.3 Path loss models

Radio wave propagation can be modelled with different path loss models. The free-space path loss (FSPL) model [58] assumes a LOS connection between two wireless communication links. The Okumura-Hata model [33] is an empirical model based on real-world measurements. However, these propagation models were constructed with data sets that were measured on the ground level. Generally, they do not take into account the receiver being higher than the transmitter. [56]

A few propagation models that are more suited for communications between a base station and drone have been researched. The 3rd Generation Partnership Project (3GPP) technical report TR 36.777 [1] introduces models for both LOS and non-line-of-sight (NLOS) conditions and for rural macro, urban macro, and urban micro (UMi) scenarios.

3.3.1 Free-space path loss model

FSPL is the attenuation of energy between isotropic antennas measured in decibels. It is dependent on the used carrier frequency and the distance between the antennas.

$$PL_{\text{FSPL}} = 32.45 + 20 \cdot \log_{10}(d_{\text{km}}) + 20 \cdot \log_{10}(f_{\text{c-MHz}}) \,, \tag{3.1}$$

where

d_{km} is distance (km), and
$f_{\text{c-MHz}}$ is frequency (MHz).

3.3.2 Okumura-Hata model

The Okumura-Hata model depends on the antenna heights, the carrier frequency, and the distance between the antennas. It measures path loss in decibels.

$$PL_{\text{O-H}} = A + B \cdot \log_{10}(d_{\text{km}}) + C \tag{3.2}$$

where A, B, and C depend on the UE antenna height (h_{UE}), BS antenna height (h_{BS}), and carrier frequency (f_{c}).

$$A = 69.55 + 26.16 \cdot \log_{10}(f_{\text{c-MHz}}) - 13.82 \cdot \log_{10}(h_{\text{BS}}) - a(h_{\text{UE}}) \tag{3.3}$$

$$B = 44.9 - 6.55 \cdot \log_{10}(h_{\text{BS}}) \tag{3.4}$$

The factor C and the function $a(h_{\text{UE}})$ are dependent on the environment. For rural areas:

$$C = -4.78 \cdot [\log_{10}(f_{\text{c-MHz}})]^2 + 18.33 \cdot \log_{10}(f_{\text{c-MHz}}) - 40.98\,, \tag{3.5}$$

$$a(h_{\text{UE}}) = (1.1 \cdot \log_{10}(f_{\text{c-MHz}}) - 0.7) \cdot h_{UE} - (1.56 \cdot \log_{10}(f_{\text{c-MHz}}) - 0.8)\,, \tag{3.6}$$

where

d_{km} is distance (km),
$f_{\text{c-MHz}}$ is frequency (MHz),
h_{UE} is UE height (m), and
h_{BS} is BS height (m).

Table 3.1. *Range of validity of the Okumura-Hata model [42].*

distance	d_{km}	1–20 km
frequency	$f_{\text{c-MHz}}$	150–1500 MHz
UE height	h_{UE}	1–10 m
BS height	h_{BS}	30–200 m

Table 3.1 describes the range of validity for the Okumura-Hata model. Even though the Okumura-Hata model is widely used in radio network planning, it is not suitable for drone to base station path loss estimation. Both the UE height and the distance ranges are too limited for that purpose. With UE heights of 50–150 m, the term $a(h_{\text{UE}})$ would decrease the overall path loss to negative values. As a result, without any adjustments to the path loss model, it is only suitable for measuring the path loss on the ground level for comparison

purposes. Normally, for UE heights of 1.5–10 m, $a(h_{\mathrm{UE}})$ is in the range of 2.5–21. By removing the effect of $a(h_{\mathrm{UE}})$, the path loss model can be adjusted above the FSPL model. However, without the full effect of UE height to the overall pathloss, the validity of this modification is questionable.

3.3.3 COST Hata model

The European cooperative for scientific and technical research (EURO-COST) [10] extended the Okumura-Hata model to cover the frequency range 1.5–2 GHz. This is accomplished by adjusting the parameters in equation 3.3 to the following:

$$A = \mathbf{46.3} + \mathbf{33.9} \cdot \log_{10}(f_{\text{c-MHz}}) - 13.82 \cdot \log_{10}(h_{\mathrm{BS}}) - a(h_{\mathrm{UE}}) \tag{3.7}$$

3.3.4 3GPP Technical Report model

The path loss model introduced by the 3GPP technical report [1] is dependent on the UE height h_{UE}, the 3D distance between the UE and base station, and the carrier frequency f_{c}. Figure 3.2 depicts the various heights and distances. The UE height h_{UE} can be larger, equal, or smaller than the base station height h_{BS}. The 3D distance d_{3D} can be calculated as follows:

$$d_{\mathrm{3D}} = \sqrt{(d_{\mathrm{2D}})^2 + (h_{\mathrm{UE}} - h_{\mathrm{BS}})^2} \tag{3.8}$$

For the majority of the cases, d_{3D} is very close to d_{2D}, since $d_{\mathrm{2D}} >> |(h_{\mathrm{UE}} - h_{\mathrm{BS}})|$.

For rural macro areas, in LOS conditions, the path loss in decibels is:

$$\begin{aligned} PL_{\text{RMa-LOS}} = {} & \max(23.9 - 1.8 \cdot \log_{10}(h_{\mathrm{UE}}), 20) \cdot \log_{10}(d_{\text{3D-m}}) \\ & + 20 \cdot \log_{10}\left(\frac{40\pi f_{\text{c-GHz}}}{3}\right). \end{aligned} \tag{3.9}$$

According to [1], for rural macro areas, the LOS probability is 100%, when the aerial UE height h_{UE} is between 40 m and 300 m. Table 3.2 shows the applicability range of the 3GPP path loss model for RMa LOS. However, as evidenced by the next section, it closely resembles the FSPL at certain UE and BS heights.

Table 3.2. *3GPP path loss model applicability range for RMa LOS [1].*

distance	d_{2D}	≤10 km
UE height	h_{UE}	10…300 m

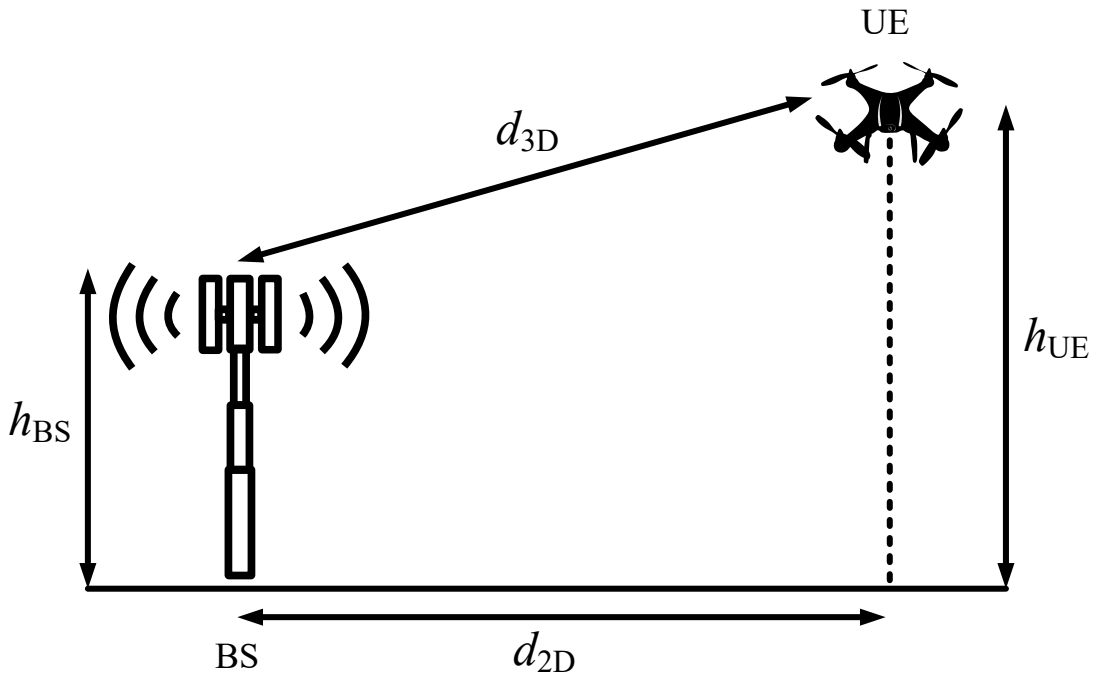

Figure 3.2. *2D and 3D distances for aerial UEs.*

3.3.5 Path loss model comparison

Even thought the validity of these four models is not defined for the same conditions concerning distances, heights, and frequencies, it is still of importance to compare how they model the path loss between a drone and a base station. These calculations assume the following parameters:

d_{2D} = 1–30 km,
h_{BS} = 60 m,
h_{UE} = 100 m, and
f_c = 800 MHz or 1800 MHz .

Figure 3.3 depicts the behaviour of the four path loss models in regards to distance between the UE and the BS for carrier frequencies f_c = 800 MHz and f_c = 1800 MHz. The FSPL and the 3GPP model behave very similarly with these parameters. That is to be expected, since the probability of a LOS connection is high with an UE height of 100 m and with a base station height of 60 m. The modified Okumura-Hata and COST Hata models have been adjusted by removing the effect of UE height to the overall pathloss.

3.4 Key performance indicators

Key performance indicators (KPI) for cellular networks are used to optimise and monitor the performance of the network. Additionally, these performance metrics are used in handover procedures. The most significant KPIs in regards to this project are the downlink received power and signal quality.

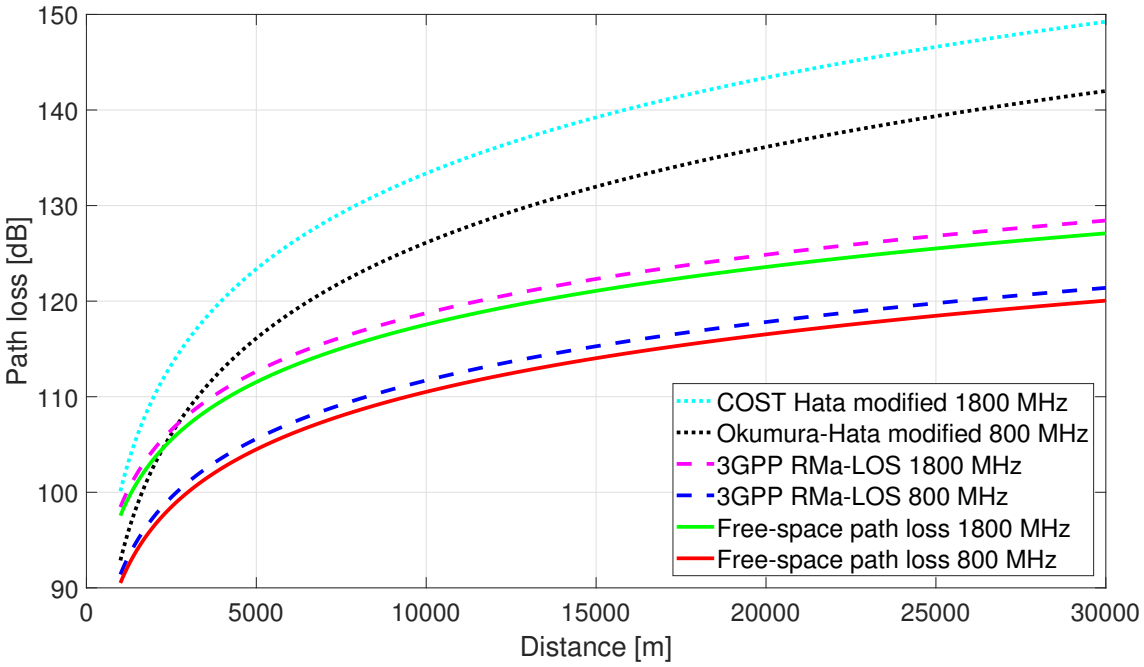

Figure 3.3. *Path loss comparison between different propagation models.*

3.4.1 Received power

For all the measured technologies (2G Global System for Mobile Communications (GSM), 3G Universal Mobile Telecommunications System (UMTS), and 4G LTE), there are different names for the received power parameter. For GSM, The signal strength KPI is defined as:

$$RX\ level\,full(\text{dBm}) = EIRP(\text{dBm}) - path\ loss(\text{dB})\,,$$

where path loss means the attenuation of the signal power between the transmitter and the receiver and effective isotropic radiated power (EIRP) is defined as:

$$EIRP(\text{dBm}) = P_{\text{TX}}(\text{dBm}) - L_{\text{cable}}(\text{dB}) + G_{\text{antenna}}(\text{dBi})\,,$$

where P_{TX} is the transmitted power, L_{cable} is the cable loss, and G_{antenna} is the isotropic antenna gain.

In 3G UMTS systems, received signal code power (RSCP) means the measured received power on a common pilot channel (CPICH) transmitted from the NodeB [35]. The word *code* is a reference to scrambling codes, which are used to differentiate cells in the downlink.

Reference signal received quality (RSRP) is the equivalent received power value for LTE networks. It is the narrowband reference signal power.

3.4.2 Signal quality

Signal quality is used to measure the quality of the downlink signal. Again, all the technologies measure this KPI in a different manner. For GSM, *RX quality full* relates to the average bit error rate (BER) for a certain time frame. The parameter E_c/N_0, used in UMTS, denotes received energy per chip divided by the power density in the band [2].

$$E_c/N_0(\text{dB}) = \frac{RSCP(\text{dBm})}{RSSI(\text{dBm})},$$

where RSSI stands for received signal strength indicator, that is, the downlink wideband received power. The LTE equivalent is the reference signal received quality (RSRQ). It indicates the quality of the reference signal.

$$RSRQ(\text{dB}) = N \cdot \frac{RSRP(\text{dBm})}{RSSI(\text{dBm})},$$

where N is the number of resource blocks. RSSI is the same wideband received power as in GSM and UMTS. It can also be stated as:

$$RSSI = \text{serving cell power + interference + noise}.$$

All the technology specific KPI values are listed in table 3.3.

Table 3.3. *KPI terms for GSM, UMTS, and LTE.*

Technology	2G GSM	3G UMTS	4G LTE
Signal strength	RX level	RSCP	RSRP
Signal quality	RX quality	E_c/N_0	RSRQ

3.5 Frequency bands and handovers

In rural areas, most of the base stations use the LTE band 20 (800 MHz), UMTS band 8 (900 MHz), or E-GSM (900 MHz). For urban areas, there are higher frequency ranges in use, such as the LTE band 3 (1800 MHz). Each of these frequency bands use frequency-division duplexing (FDD), where both the receiver and the transmitter function at different carrier frequencies. In other words, the FDD uplink and FDD downlink use different frequency ranges.

The measurements were conducted with technology locks, that is, the UE was forced to measure only the chosen radio technology (GSM, UMTS, or LTE). That meant that there were no inter-technology handovers. Moreover, even though the phone was not locked to a specific frequency range, the UE experienced only a few inter-frequency handovers in

LTE networks. As opposed to a urban environment, rural areas primarily use the lower frequencies to increase signal range.

Since the measurements were performed along a mobility route, where the drone flies a fixed path, handovers occurred mainly because the UE moved away from the coverage area of its serving cell to an area where the received signal power from another cell is higher. In most cases, handovers occur because of received signal power or signal quality measurements performed by the UE. For the purpose of these KPI measurements, the UE maintains cell lists that categorise cells based on their function. These lists are used in the handover procedures. More information about these lists can be found in the next section.

3.6 Cellular network terms

GSM cell lists

The GSM Neighbour Cell list is derived from the base station identity code (BSIC) and the BCCH Allocation (BA) list. BSIC is used to distinguish the co-channel frequency used in the neighboring cell. The broadcast control channel (BCCH) list is an index of frequencies supported on the neighbouring cells. [19]

UMTS cell lists

The cells are divided into three sets:

1. the active set includes every cell that the UE is tracking for soft handover (SHO) purposes,
2. the neighbour set includes every cell that is not in the current active list but that the UE is monitoring with measurements,
3. the detected set includes every cell that is not in either the the active set or the neighbour set but the UE has detected. [35]

LTE cell lists

Unlike in GSM and UMTS systems, the LTE network side (evolved UMTS terrestrial radio access, (E-UTRA)), does not maintain a neighbor cell list. Instead, the UE monitors detected neighbor cells and reports these to its serving eNB. [34]

Base station terminology

Figure 3.4 and table 3.4 depict all the various terms for GSM, UMTS, and LTE base stations. The top term represents the technology specific base station name. The middle term is used to distinguish different cells from each other. In UMTS, the primary scrambling code (PSC) in downlink is used to differentiate a particular cell. In LTE, the physical cell identity (PCI) is used for the same purpose.

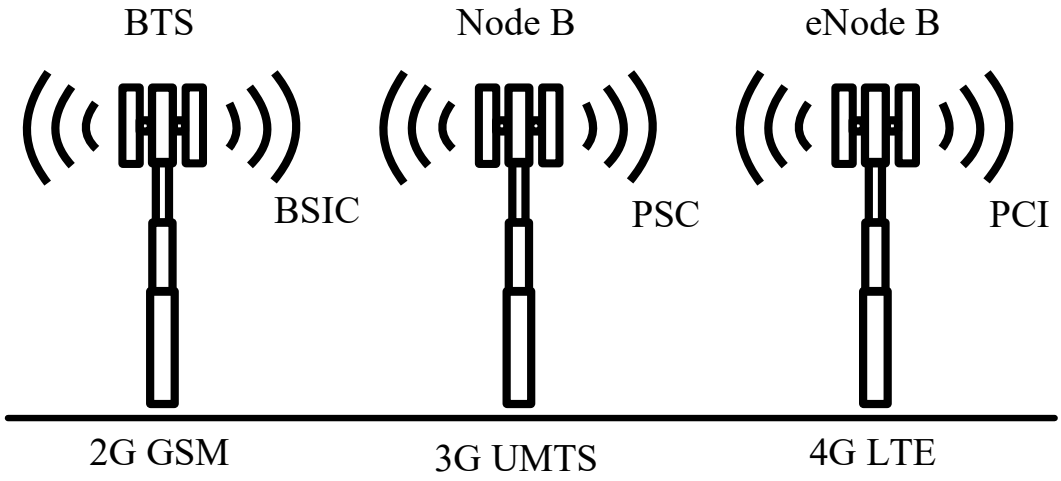

Figure 3.4. *Base station terminology.*

Table 3.4. *Base station terms for GSM, UMTS, and LTE.*

2G GSM	3G UMTS	4G LTE
Base transceiver station	Node B	Evolved Node B
Base station identity code	Primary scrambling code	Physical cell identity

4. MEASUREMENT METHODS

This chapter describes the various methods used in the measurement campaign. It includes hardware and software specifications, measurement and mission planning, site selection and various other procedures used to execute the drone measurements. These measurement methods were a significant part of the successful completion of this project. Planning, designing, and implementing the measurements laid the foundation for the whole project.

4.1 Drone introduction

The measurements were conducted using a DJI Inspire 2 [14] drone. This commercially available drone is intended for professional photographers. However, it was selected for its reliability and payload carrying capacity. For measurement purposes, a mobile phone had to be attached to the bottom of the drone. Figure 4.1 describes all the drone components.

Figure 4.1. *DJI Inspire 2 components.*

4.1.1 Drone components

The drone contains several sensors, including two inertial measurement units (IMUs) and two barometers. These sensors are used to maneuver the aircraft and to measure the drone's altitude, respectively. A built-in GPS module handles the navigation. A camera is attached to a 360° rotating gimbal. The drone also features forward, upward, and downward facing obstacle detection and avoidance sensors and a dual-battery system for added safety.

The DJI Inspire 2 has a bottom plate with some screw holes. However, it was not suitable for payload purposes without modifications. Therefore, a mounting bracket for the phone was manufactured by Tampere University of Technology (TUT) ProLab [57]. This bracket enabled to mount the phone to the drone with a quick release system similar to a bicycle phone mount. The measurement phone was equipped with a Armor-X case with the required quick release lock. This custom made mounting bracket and the phone with the protective case is shown in figure 4.2.

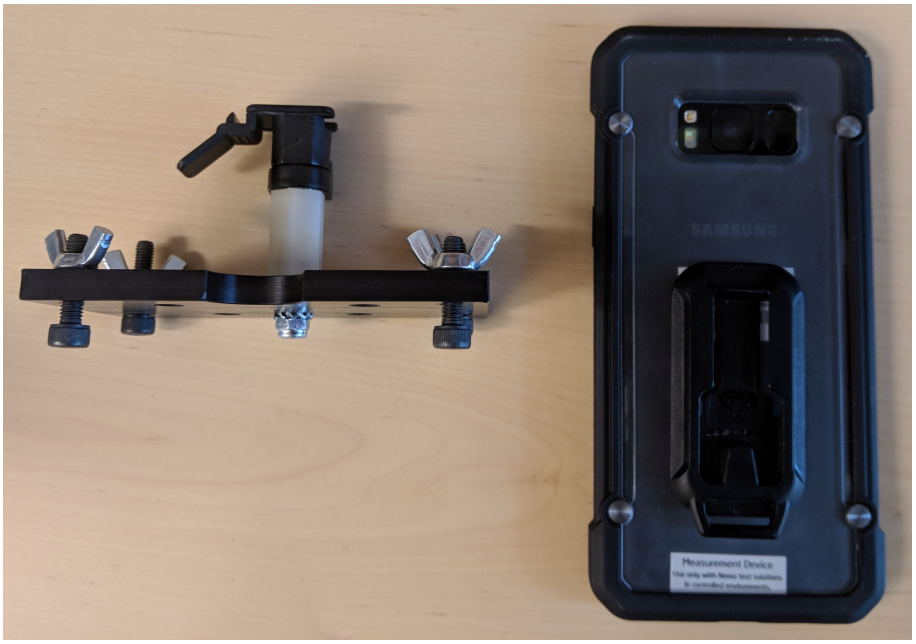

Figure 4.2. *Mounting bracket and Samsung Galaxy S8 with the Armor-X case.*

4.1.2 Drone capabilities

In addition to the payload capability, safety and reliability were the reasons for choosing this drone model for our measurements. The drone uses a combination of infrared and ultrasonic sensors for obstacle detection and avoidance. These sensors are facing forward, downward, and upward. Additionally, the dual battery system provides redundancy in case of a single battery failure.

The return to home (RTH) function of the drone was used in the measurements. Using both GPS and the downward facing visual sensors, the drone records its home spot, that is, the take-off location. After the measurement mission is over, it is both faster and more convenient to have the drone return back to the home spot on its own. Some pertinent DJI Inspire 2 technical specifications are listed in table 4.1.

Table 4.1. *DJI Inspire 2 technical specifications [14].*

Maximum flight time	27 min
Maximum takeoff weight	4250 g
Maximum speed	94 kph
Maximum wind speed resistance	10 m/s
Operating temperature	-20° to 40° C

4.2 Measurement devices and software

A Samsung Galaxy S8, running Android version 7.0, was attached to the drone and used as a measurement device. The primary measurement program was Nemo Handy Handheld Measurement Solution. This program requires custom firmware on an Android device to work.

4.2.1 Bluetooth headset

The project examined two different ways to implement the connection between the phone attached to the drone and the repair worker on the ground. One solution was to use a Bluetooth headset to enable a voice connection. A phone call could be accomplished by either a redial function or by voice commands such as Google Assistant. According to our tests, a reliable Bluetooth connection was feasible as long as the range was under 100 meters and the headset had a line-of-sight connection to the drone. Another option is to use the phone that is connected to the drone as a mobile Wi-Fi hotspot. This enables a phone on the ground to have a data connection. Additionally, using Voice over Wi-Fi (VoWiFi) technology, this method enables to have a regular voice connection over the wireless network as well.

4.2.2 Nemo Handy Handheld Measurement Solution

Nemo Handy Handheld Measurement Solution [45] made by Keysight Technologies is a drive test and measuring tool for wireless networks, including cellular networks. During the drone flight, the program monitors various parameters about the state of the cellular network. These measurements are saved to the flash storage of the Samsung Galaxy S8. In order to gain access to some of the network information, the phone is running a custom firmware [50]. Nemo Handy has a lot of features ranging from application testing to voice quality testing. However, the most significant feature is its ability to lock to a particular system (GSM, UMTS, LTE), frequency band, or to a specific scrambling code in UMTS or to a PCI in LTE. When a specific technology lock is activated, the phone will only collect data, for that particular cellular technology. All the measurements were performed with the UE locked to either a 2G, 3G, or 4G technology.

4.2.3 G-NetTrack Pro

G-NetTrack Pro [28] made by Gyokov Solutions is a similar drive test tool used for radio network planning and optimization. Compared to Nemo Handy it has some limitations because it does not have kernel level access to certain interfaces. However, for certain functions, G-NetTrack Pro provides better information than Nemo Handy. Additionally, it does not require an additional program to export the measurement results as a text file. Furthermore, the program generates keyhole markup language (KML) files that can be used with Google Earth Pro [30] to visualize the measurement results. Figure 4.3 shows screenshots of both measurement programs.

4.3 Flight software

Flight software for drones is used for the command and control of the aircraft. Both flight software were run on an Apple iPad mini 4 tablet connected to the remote controller (RC) of the drone. Figure 4.4 shows the tablet connected to the remote controller.

4.3.1 DJI GO 4

The *DJI GO 4* application is the manufacturer recommended flight software for manual command and control of the drone. However, its autonomous flights features are not as well developed. Therefore, all the measurement flights were performed with the Litchi application. DJI GO 4 was used for learning how to fly the drone, experimenting with the settings, and conducting shorter test flights. This program was also used to update the firmware of all the drone components (aircraft, remote controller, camera, and batteries) and to calibrate the compass and the IMU of the drone. A screen capture of the DJI 4 GO application is shown in figure 4.5.

(a) *Nemo Handy.* ***(b)*** *G-NetTrack Pro.*

Figure 4.3. *Measurement software.*

Figure 4.4. *iPad mini 4 tablet connected to the remote controller.*

4.3.2 Litchi for DJI Mavic / Phantom / Inspire / Spark

The *Litchi for DJI Mavic / Phantom / Inspire / Spark* application was used for autonomous flights. It is accompanied by a mission planning website, where detailed autonomous drone missions can be designed using a Google Earth based map tool. These missions are

synchronised to the flight software running on a smart device. More information about mission planning can be found in section 4.4.4. Figure 4.6 shows the Litchi application running on the tablet.

Figure 4.5. *DJI GO 4.*

Figure 4.6. *Litchi for DJI Mavic / Phantom / Inspire / Spark.*

4.4 Measurement plan

The project started by applying for the necessary permits concerning raising a cell phone to the sky and measuring cellular networks. The second step was to determine the local flight restrictions about drone flight altitudes and restricted fly zones. The next step was to determine appropriate sites for conducting the measurements. After that, it was time to plan the missions in terms of measurement parameters and execution. The last step was to plan the autonomous flights.

4.4.1 Local legislation, permits, and flight restrictions

Because using a drone for scientific purposes is not categorised as a hobby activity, it was classified as a professional drone operation. For that reason, complying with the regulations set by the Finnish Transport Safety Agency (Trafi) [25] was mandatory. The regulation OPS M1-32 [26] governs the use of remotely piloted aircraft (RPA) in Finland. These regulations dictate the minimum requirements of a professional drone operation:

1. Register as a drone operator.
2. Have an insurance against third party damage.
3. Apply a sticker with a name and contact information to the drone.
4. Keep a flight journal for all the flights.

The flight journal entails details about every flight, such as time, location, weather, purpose, and description about any problems or mishaps. The journal has to be stored for a minimum of three years. Additionally, the guidelines require a safety assessment and procedures document that involves identifying and assessing possible risks and how to behave in an emergency situation. The safety guidelines and preflight checklist is in appendix B.

In Finland, it is illegal to use an unlicensed radio transmitter, such as a mobile phone, in an aerial vehicle. The Finnish Communications Regulatory Authority (FICORA) [21] issued a radio permit for TUT for the use of measuring cellular networks with a drone. Additionally, the mobile network operator (MNO) Elisa Oyj [17], gave permission to use their cellular network for the measurements.

There are restrictions on both the allowed flight altitudes and geographical areas on where to fly a drone. These no-fly zones are meant to secure critical infrastructure, such as, power plants, military bases, and oil refineries [22]. Furthermore, there are special control zones near airports [48]. Figure 4.7 depicts the control zones for the Tampere-Pirkkala Airport. The color codes are explained in table 4.2.

4.4.2 Technologies and frequency bands

In order to evaluate the differences between various cellular network technologies, the measurements were conducted on Elisa's 2G GSM, 3G UMTS, and 4G LTE networks. The

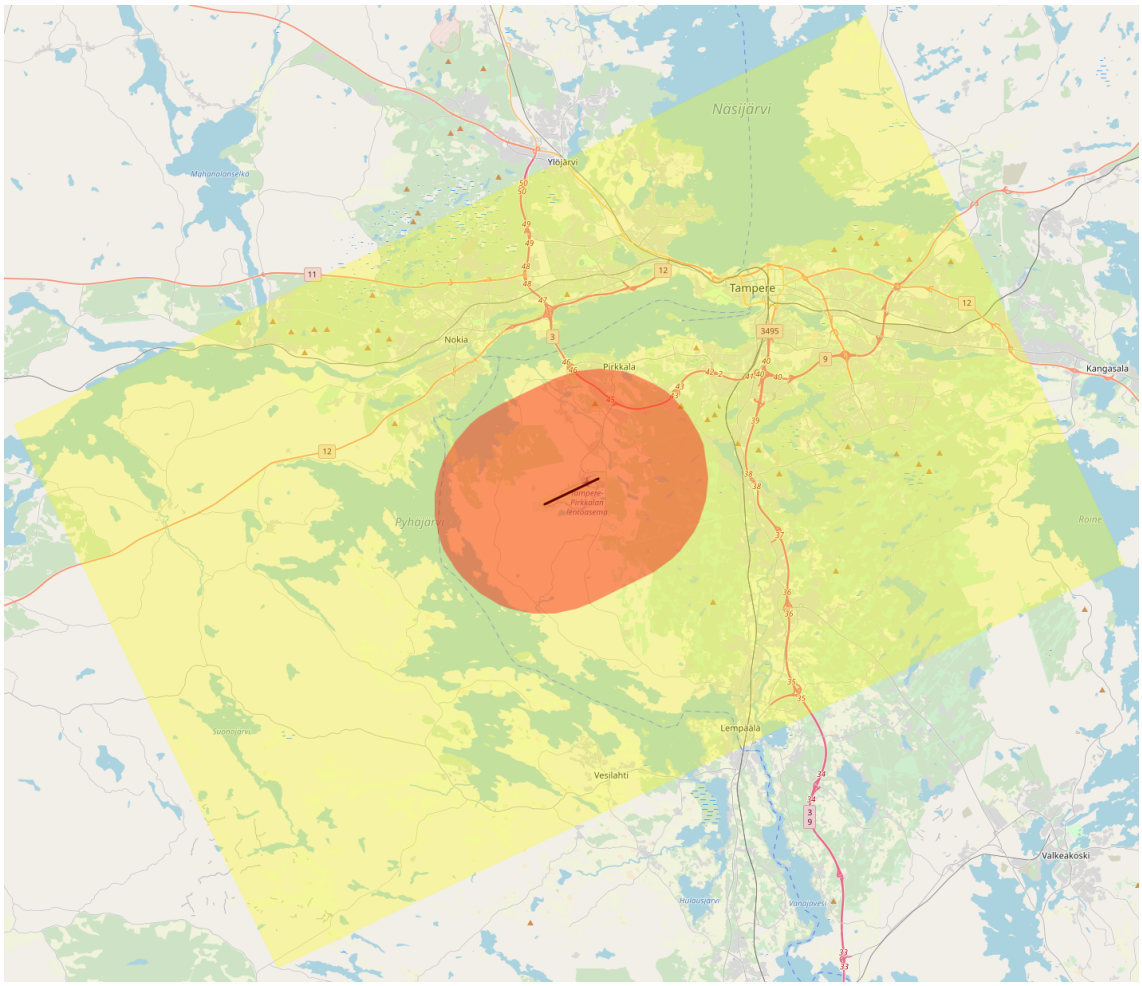

Figure 4.7. *The control zones for the Tampere-Pirkkala Airport [55].*

Table 4.2. *The control zone color codes.*

Color code	Flight restrictions
Red	Only with permission from the air traffic control
Yellow	Maximum drone altitude: 50 m
Elsewhere	Maximum drone altitude: 150 m

measurement software, Nemo Handy, is capable of locking to a single system to narrow the measurements to a desired technology. Since the measurement locations were in rural areas, most of the measured frequency bands were either 800 MHz (LTE) or 900 MHz (GSM, UMTS). In some areas, the UE connected to LTE 1800 MHz base stations as well. The used frequency bands are shown in table 4.3.

4.4.3 Site selection

The criteria for selecting appropriate measurement locations were given by the project partner, Elenia. These principles were selected to simulate the conditions of an actual electrical grid repair situation. The most important criteria for site selection were:

1. Sparsely populated area.
2. Next to a 20 kV or a 110 kV overhead power line.
3. Safe to fly.
4. No risk to people, animals, or to the environment.

Additionally, the locations had to reside outside the Tampere-Pirkkala Airport control zone depicted in figure 4.7, in order to fly at altitudes of over 50 meters. Furthermore, the measurement sites had to have a relatively easy access by car and had to be at a reasonable travel distance. The sites were selected primarily with the help of Google Maps [31], Google Earth Pro [30], and Fingrid's electric grid map service [24]. Using these tools, the goal was to find a large, remote, and open area that was close to an overhead power line. The site also had to be accessible by a car, which ruled out privately owned land behind a gate or a barrier. Most of the selected sites were a few year old tree harvesting areas. The measurement locations and the Airport control zone are shown in figure 4.8 and the measurement dates and coordinates are described in table 4.4.

The measurement locations were named after the nearest municipality or village. Some prior research was conducted about possible nearby base stations for each measurement site. However, because the data concerning base station locations, cell orientation, or antenna height is not public, base station location data was not used in site selection. Due to the fact that all the locations are in rural areas, the base station antenna heights have been assumed to be between 50 m and 70 m, which is commonplace in sparsely populated areas. Because the physical implementation of the cellular network varies between the measurement locations, comparing for example path loss results between different sites is not suitable. However, having five various spots with differing environments will allow to draw limited conclusions about the measurement results.

Table 4.3. *Measured frequency bands.*

Technology	Frequency band
GSM	900 MHz
UMTS	900 MHz
LTE	800 MHz
LTE	1800 MHz

Table 4.4. *Measurement locations, dates, and coordinates.*

Location	Date	Latitude	Longitude
Pinsiö	31.5.2018	61.576617	23.455424
Valkeakoski	13.6.2018	61.237533	24.166493
Orivesi	20.6.2018	61.612329	24.187912
Nokia	27.6.2018	61.516498	23.435078
Savonkylä	10.7.2018	61.687474	24.014687

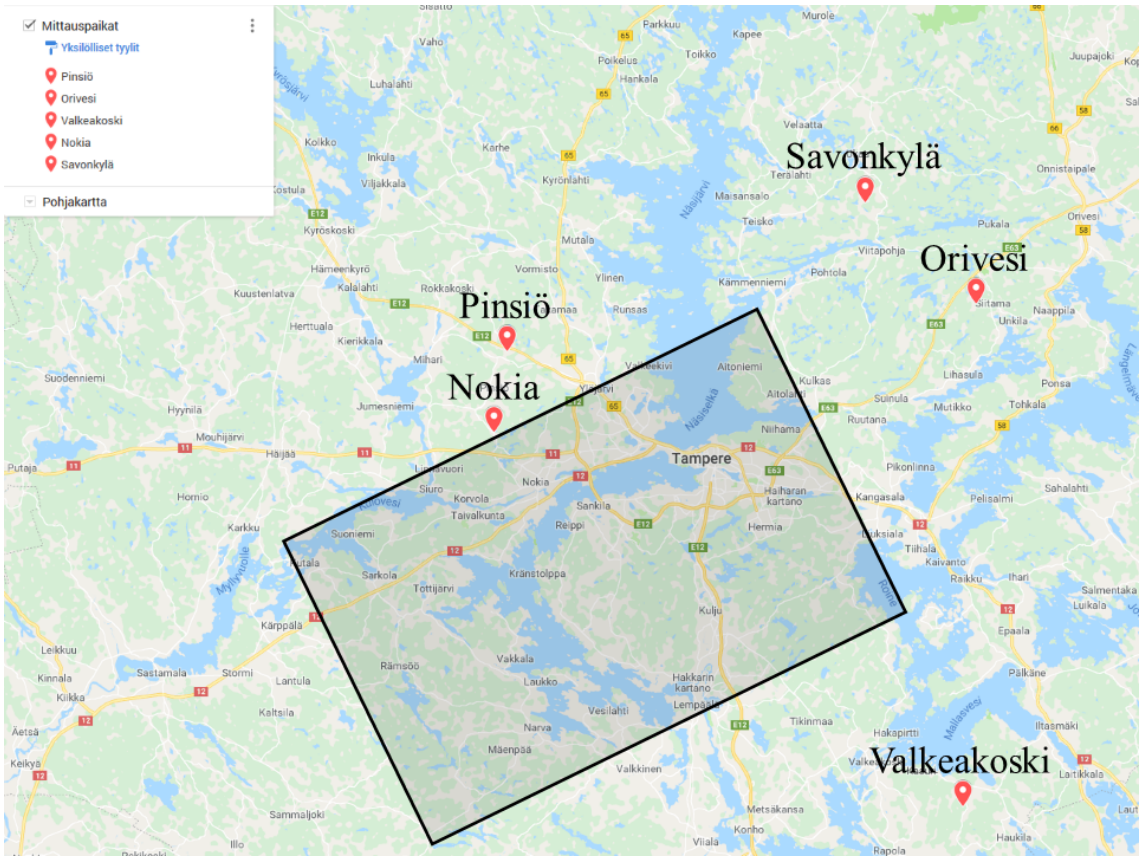

Figure 4.8. *Measurement locations.*

4.4.4 Mission plan

Instead of doing measurements in the same position at various altitudes, the drone flew a mobility route around the measurement site. The reason for that was to establish a connection to as many base stations as possible. In order to have reproducible and comparable measurements, it was necessary to perform these mobility routes as autonomous flights. These flights were designed with the *Litchi Mission Hub*, a Google Maps based mission planner. The missions were planned to last about four to five minutes and to be approximately one kilometre in length. The biggest restricting factor in terms of flight time was the limited battery life. There were four pairs of batteries in use and a single flight would drain about 20%–30% battery depending on altitude, wind speed, temperature, and the time spent on ascending to the mission altitude as well as landing the drone.

After finding a suitable location, the flight route was designed by inserting waypoints with the desired altitude to the Google Maps satellite image. Additionally, the Litchi mission planner enables to change various flight parameters, such as flight speed, drone heading, curve size, and camera functions. Furthermore, the choice of a home point (that is, the drone take off and landing point), was important in order to have a constant visual line-of-sight to the drone. The regulations dictate that either the pilot or a spotter must have VLOS to the drone at all times. Figure 4.9 depicts the Litchi Mission Hub.

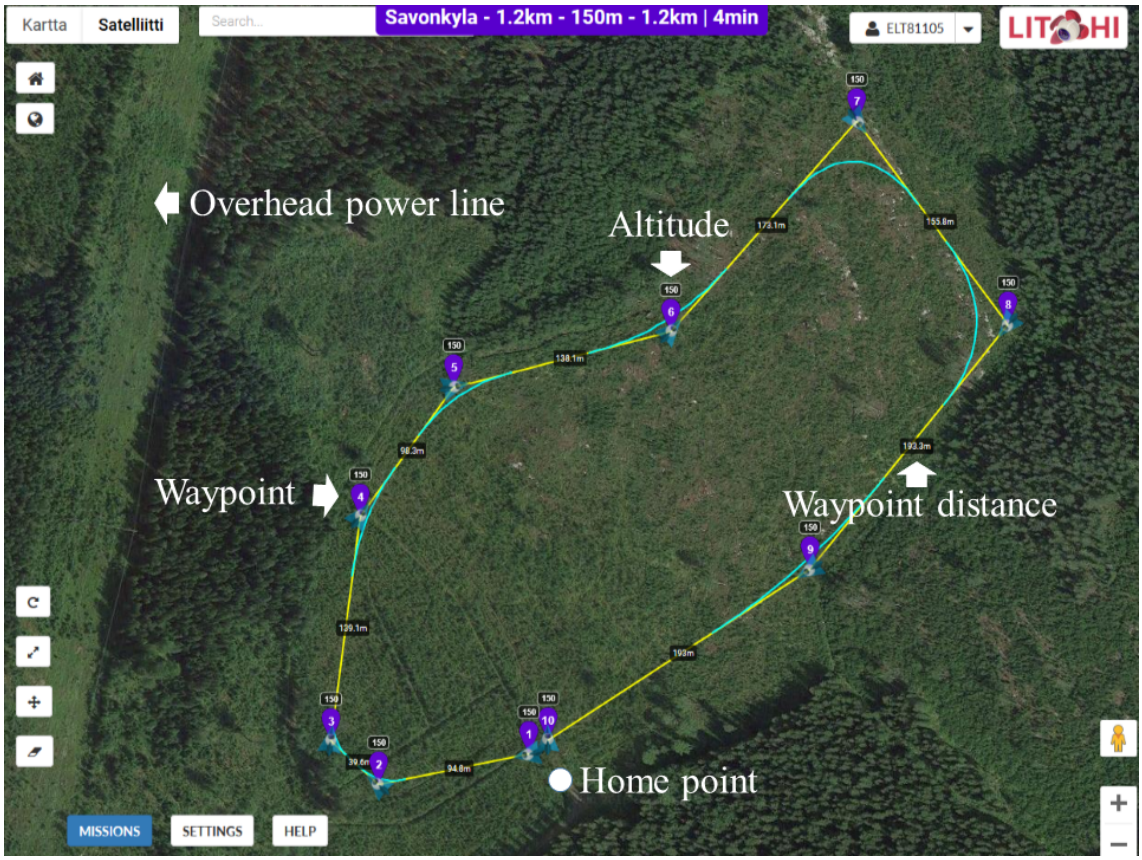

Figure 4.9. *Litchi Mission Hub [40].*

4.4.5 Flight plan

To test the effect of drone altitude to the measured KPI parameters, the same flight route was flown at altitudes of 50 m, 100 m, and 150 m. These altitudes are in relation to the ground level of the first waypoint, which means that the drone's distance to the ground during the flight route varies based on land elevation. Due to the fact that the corresponding route on the surface was often inaccessible by car or on foot, the measurements were not repeated at ground level. However, limited measurements were gathered at the home point when the phone was at an altitude of 1.5 m. All the flight routes were repeated for each technology (GSM, UMTS, and LTE), which equals nine measurement flights in each location for a total of 45 flights. Some additional flights were flown for added data and testing purposes, but they are not considered in the results. Figure 4.10 shows an example of the actualised flights in the Savonkylä location. The green line represents the 50 m flight route, the yellow line is the 100 m flight route, and the red line illustrates the 150 m flight route.

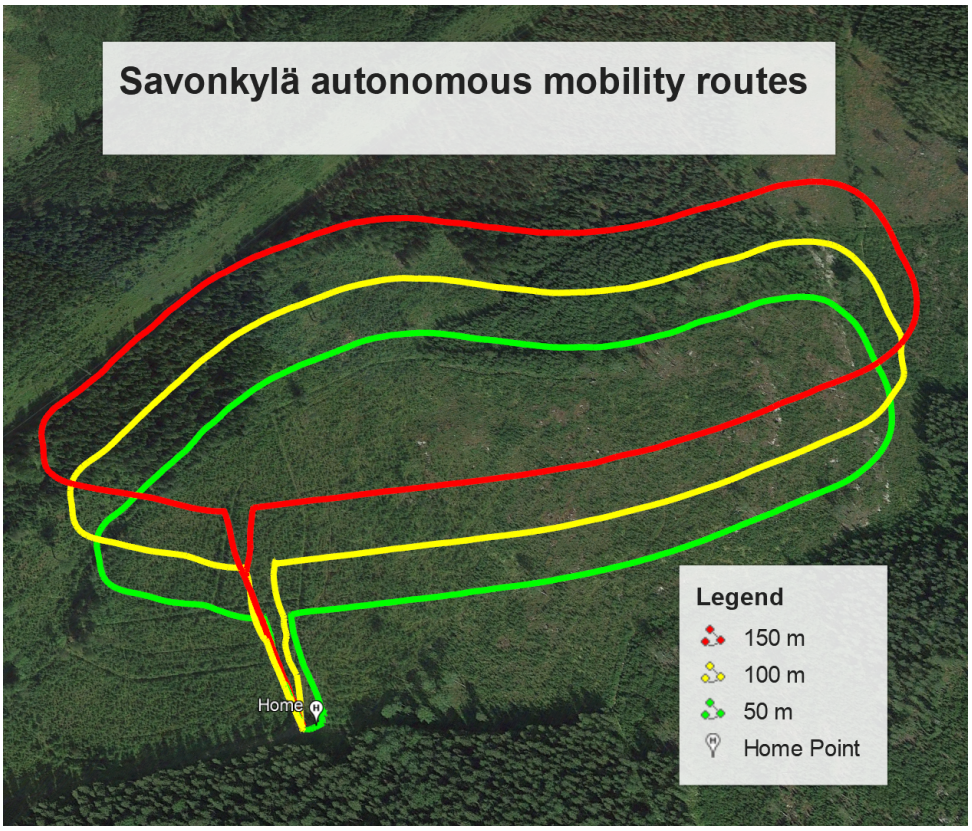

Figure 4.10. *Autonomous flight routes.*

4.5 Measurement sequence

The measurement sequence followed this order:

1. Make a flight notification using the *Droneinfo* application [15].
2. Scout the area for possible risk factors (trees or other obstacles near the flight route).
3. Decide the home point location with a VLOS to the flight route.
4. If necessary, clear debris and vegetation to guarantee a safe landing zone.
5. Secure the landing pad to the ground.
6. Assemble the drone (batteries, mounting bracket, camera, and propellers).
7. Connect the tablet to the remote controller.
8. Make sure everything is properly seated.
9. Power up the RC and the drone, and launch the flight software.
10. Calibrate the compass if necessary.
11. Make sure that the drone has GPS connectivity and that the RC is connected to the drone.
12. Fly a short test flight to ensure everything is working properly and that the settings are correct.
13. Configure the measurement software (Nemo Handy or G-NetTrack Pro) and start the measurements.
14. Attach the phone to the drone.

15. Fly the first 4G measurement at a 150 m altitude by starting the autonomous mission.
16. Land the drone, power it down, and detach the phone.
17. Stop the recording and save the measurements to the phones internal storage.
18. Change the batteries after three flights.
19. Restart the measurement, attach the phone to the drone and power it up.
20. Repeat steps 15–19 for all the altitudes and technologies for a total of nine flights.
21. Dissemble and pack everything to the carrying case.

The Droneinfo application, made by Trafi, provides information about maximum flight altitudes, restricted areas, and no drone zones. Currently, the flight announcement is not mandatory, but it will alert other drone pilots about your flight duration, location, and maximum altitude. Sometimes, due to a human error or an incorrect drone setting, flights had to be aborted and repeated. Usually, one pair of batteries was enough to complete all three measurement flights in a single technology. After the measurement was complete, the measurement files were named with a prefix (location) and a suffix (measurement ID). The date and time of the flight was also added to the file name. For redundancy, manual records of flights were kept as well. Additional information about data handling is in section 5.4. A more detailed preflight checklist and safety guidelines can be found in appendix B.

5. DATA COLLECTION AND PROCESSING

This chapter describes data collection methods for flight data, cellular network data, and base station locations. Additionally, it portraits various data manipulation methods for structuring, renaming, organising, and filtering of the original measurement data.

5.1 Flight data collection

The primary way for retrieving flight telemetry data was using the *Airdata UAV* website [3]. It is used for drone data and flight analysis. The flight logs collected by either the DJI 4 GO or the Litchi flight application are synchronised to the Airdata UAV service. Additionally, the drone collects detailed flight logs to its microSD card. This data can be retrieved by the *DJI Assistant 2* software.

5.1.1 Airdata UAV

Airdata UAV processes the log files and organises and visualises the data to an easily understood format. This telemetry data includes information, such as battery info, altitude, flight time, temperature, flight distance, GPS data, and sensor data. However, the most important feature is the ability to download this data in a CSV format for further analysis. There is also an option to download the flight route as a KML file to use with Google Earth. Figure 5.1 shows a screenshot of the Airdata UAV service.

5.1.2 DJI Assistant 2

DJI Assistant 2 is used for updating the firmware of the drone components and flight data visualisation and retrieval. Compared to the logs generated by the flight software, it provides much more detailed information at a higher sampling frequency. This data contains more comprehensive IMU information. Its primary purpose is to act as a black box in case of accidents or drone malfunctions. Therefore, the additional data is not relevant for the purposes of this project. Furthermore, the log files created by the drone are in a proprietary format that requires additional software to convert into a CSV file.

5.2 Cellular network data collection

Cellular network KPI data was collected with two drive test tools for measuring wireless networks: Nemo Handy and G-NetTrack Pro. Both programs record a number of parameters and produce text files for further analysis.

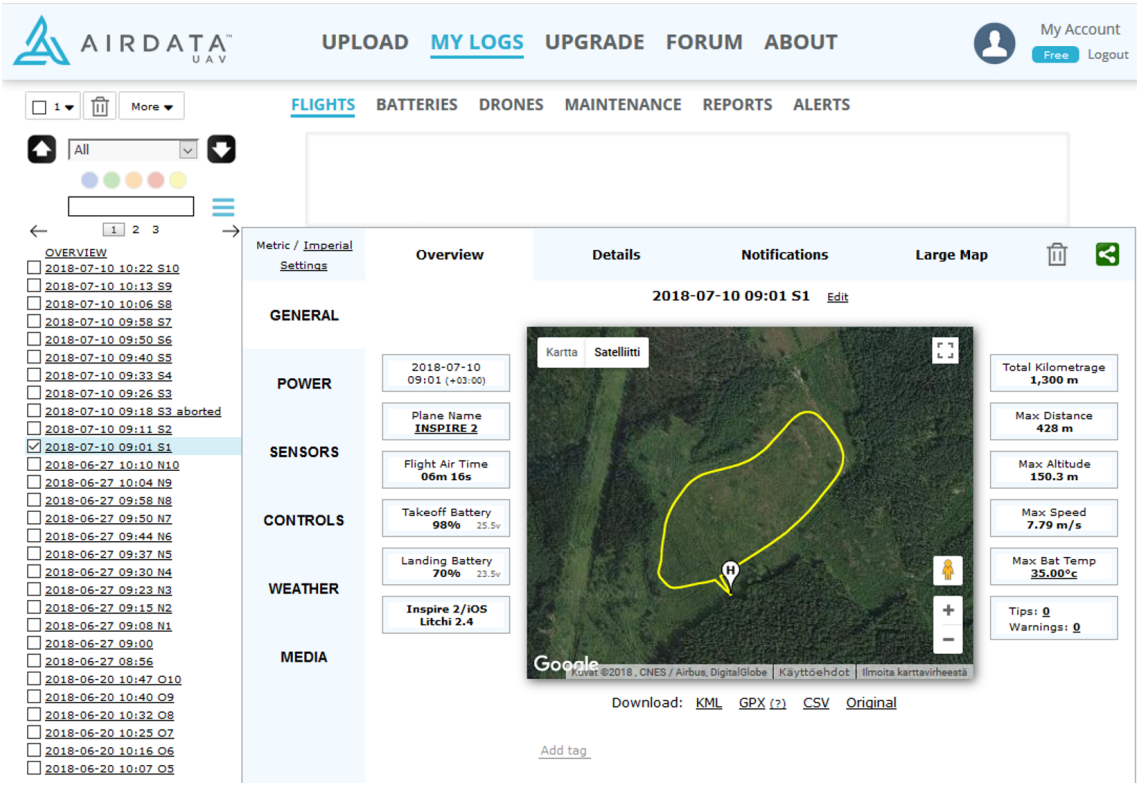

Figure 5.1. *Airdata UAV flight log service.*

5.2.1 Nemo Handy

Nemo Handy has several options for measuring cellular networks. It can lock into a specific technology, frequency band, or a PCI in LTE or a scrambling code in UMTS. Since the information about different base stations and handovers was of interest, the phone was locked to use either GSM, UMTS, or LTE for the duration of a single flight. Because this lock forces the phone to only use a particular technology, the setting effects the other measurement program as well. Figure 5.2a depicts the system forcing settings of Nemo Handy.

5.2.2 G-NetTrack

G-NetTrack is a more streamlined measurement application than Nemo Handy. Its primary function was to act as a secondary source of information for redundancy purposes. Additionally, in some cases, it offered better information about base station identification data. Another useful feature is the automated creation of KML files for displaying the measured values visually. The visualisation of serving base stations can be found in the results section in figure 6.2. Figure 5.2b depicts the drive test tab of G-NetTrack Pro.

5.3 Determining base station locations

Due to the fact that the base station data concerning location, sectors, and antenna height is proprietary information, other means of determining the base station sites had to be explored.

(a) *Nemo Handy LTE lock.* ***(b)*** *G-NetTrack Pro drive tab.*

Figure 5.2. *Drive test tools.*

This project used three tools for discovering the base station locations: CellMapper [9], Google Earth Pro, and a mast map [37].

For the base station location data, G-NetTrack Pro provided better information than Nemo Handy. Nemo Handy uses a long cell ID (LCID) while G-NetTrack records the data using a short cell ID (CID) for GSM cell identification. The LCID contains information about both the RNC (Radio Network Controller) and the CID [49]. To obtain the Cell ID, the following calculation is required:

$$CID = LCID \bmod 65536\,.$$

5.3.1 CellMapper

CellMapper is a crowdsourced service for locating base stations in 2G, 3G, and 4G networks. Using an application on their mobile device, end users collect cellular network data to be sent to the CellMapper servers. This user collected data is utilized to approximate base station locations and their coverage. The service also estimates cell directions. The accuracy of these base station locations depends on the technology, amount of user contributions, and the area type. Nowadays, most users primarily use LTE networks, which means the majority of the collected data is from 4G base stations. This results in 4G base station locations usually being more accurate than the location of 3G or 2G base stations. Additionally, rural locations with fewer obstacles between the phone and the base station has more accurate location data than urban areas. [9] Figure 5.3 shows an example of the CellMapper service.

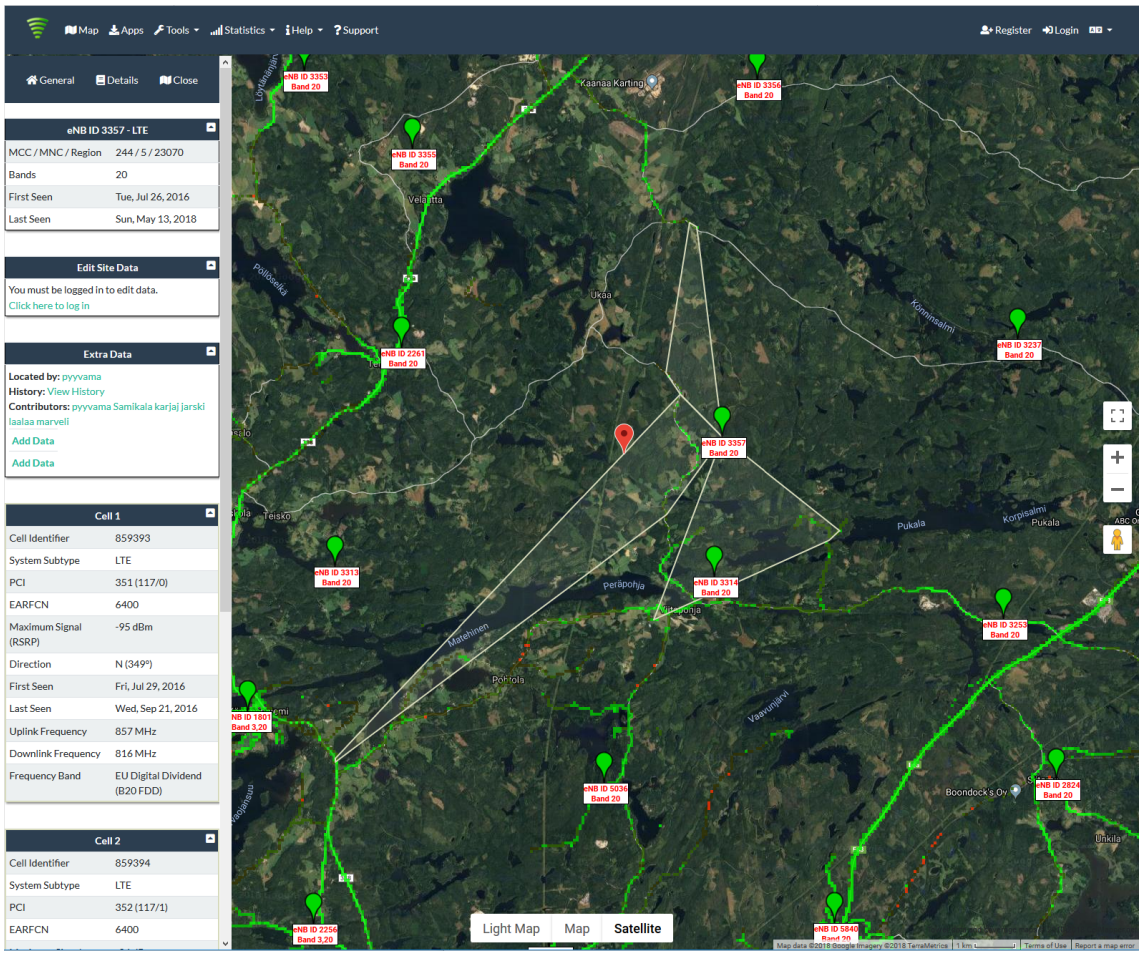

Figure 5.3. *CellMapper, a base station location service.*

The process of determining the base stations that the measurement phone was connected to, was different for each technology. For LTE networks, only the eNB ID was required to locate the base station. As for UMTS networks, two pieces of data was needed to pinpoint the base station location. CellMapper has a ”Tower Search” function that searches with the technology specific base station ID (BTS ID, NB ID, or eNB ID), and a ”BSIC/PCI/PSC Search” (Base Station Identity Code, Physical Cell Identity, Primary Scrambling Code) function that lists all the base stations associated with the searched parameter. Using either of the these search functions and narrowing the search results with the other parameter, determining the base station locations was relatively straightforward. In rare cases, where CellMapper did not have sufficient data or the indicated position was not realistic, those base station locations would be omitted from the results.

For GSM networks, however, the method was not as simple. Neither measurement program recorded the BSIC data. Therefore, 2G base stations had to be found only with the BTS ID. This was performed with a trial-and-error method. After inputting a BTS ID number, CellMapper would provide a list of all the base stations that correspond to that number. The most likely choice was determined by manually checking the location of each base station. Again, if CellMapper did not provide reliable data, the results would be ignored.

5.3.2 Google Earth Pro and a mast map

To verify the results of the CellMapper base station locations, both Google Earth Pro and a mast map was used as a verification method. The mast map was used to verify that the base station locations were located on a mast position. Since the majority of base stations in rural areas are located in masts, it is reasonable to assume that if the base station coordinates provided by CellMapper are very close to a mast site, the actual antenna location resides in that mast. Google Earth Pro was used as a third layer of redundancy to visually check if the satellite image of the place in question contains a base station.

5.4 Data processing

The post-processing and manipulation of the measured data was necessary for many reasons. Firstly, the data gathered by Nemo Handy was in a proprietary format that had to be converted to a file format that could be processed and analyzed. Additionally, a template was applied to filter all the unnecessary fields out of the measurement data to accelerate the post-processing procedure. Secondly, there were at least three different sources of data for each measurement (Nemo Handy, G-NetTrack Pro, and the flight telemetry data from Airdata UAV) that all used different parameter naming schemes, time zones, and file name structures. To easily identify which result belonged to which flight, we used a unique flight identifier to categorise each file. Finally, Matlab was used for data processing and visualisation.

5.4.1 Nemo Outdoor

Similarly to Nemo Handy, Nemo Outdoor is also a drive test tool for desktop computers and laptops. It can export the Nemo file format (NMF) formatted measurement files to CSV files. It can also analyse the measurement files with different workspace options. Figure 5.4 illustrates the analysis part of the program.

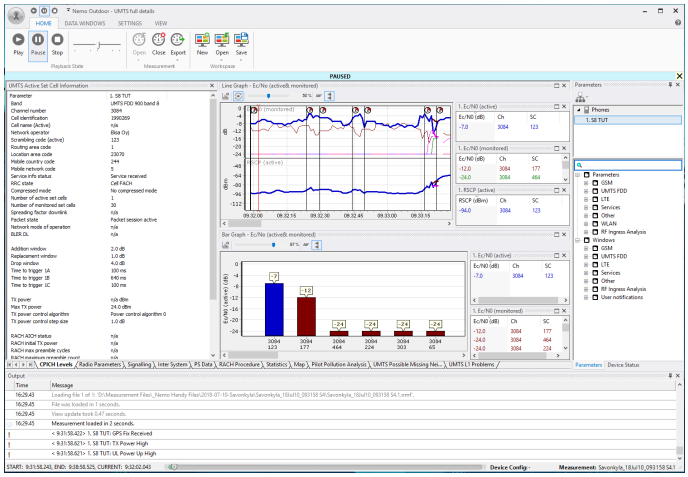

Figure 5.4. *Nemo Outdoor analyser.*

The amount of data fields in the original NMF files is immense. There are 2321 variables in the full measurement logs. These variables include fields for a great number of wireless technologies. However, the vast majority of these fields are empty. In order to limit the amount of data to only the necessary fields, a template was applied to the full measurement file. This template went quite a number of iterations based on the results individual fields provided. Initially, it included almost every cellular network parameter but ultimately, it was reduced to only 22 fields. Figure 5.5 shows the template variables.

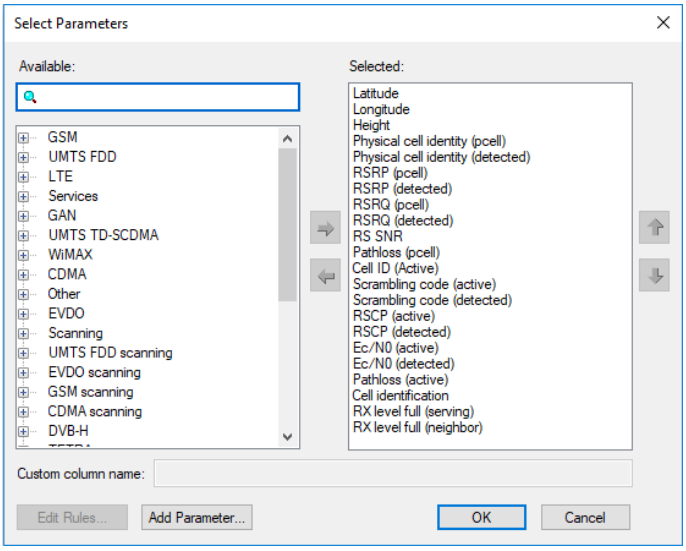

Figure 5.5. *Nemo Outdoor template parameters.*

5.4.2 Matlab

Matlab was an important tool in restructuring, organising, processing, and visualising the data. The first step was to read the CSV files to data structures. Some of the fields were split or renamed for the sake of consistency. Additionally, the time zones had to be adjusted to local time and the date and time format was unified. The data structures were then split into smaller subsets (for example, ground data and waypoint data) for better accessibility. The flight altitude and the measured technology were extracted from the data and added as modifiers. Finally, after a lot of organising and processing, every measurement set was saved as a MAT (a file format used by Matlab) file with the appropriate file identifier.

5.4.3 Data processing overview

Figure 5.6 depicts the data processing flowchart and figure 5.7 shows the flowchart of determining base station locations. These processes were refined and iterated multiple times to streamline the efficiency of data collection and processing.

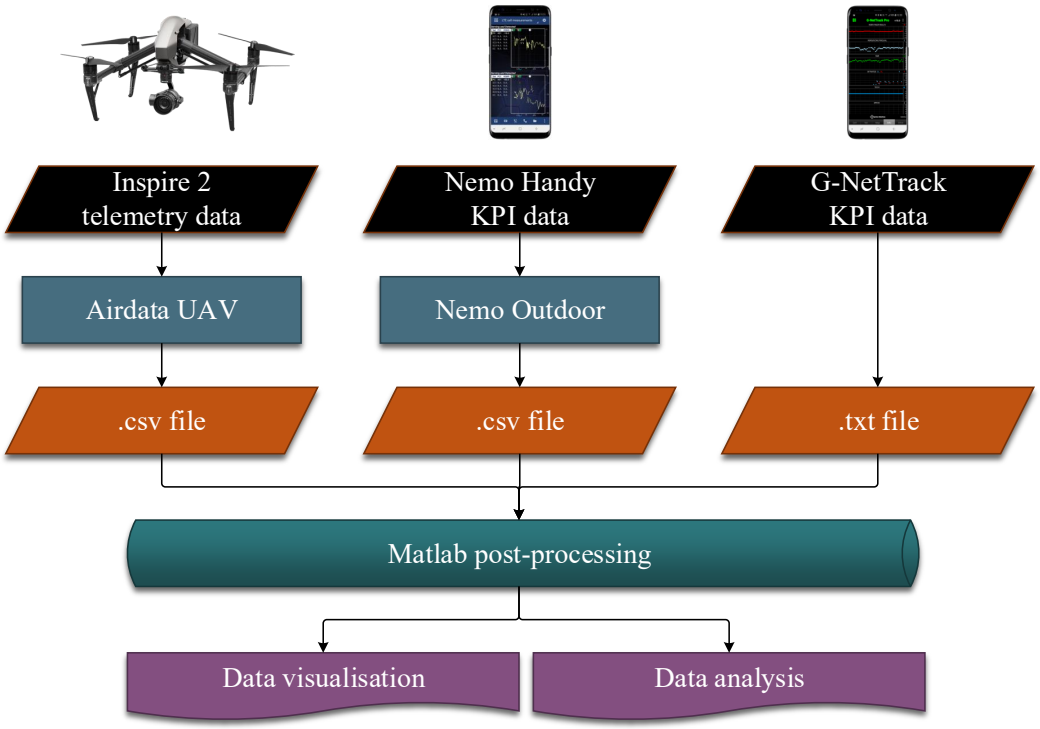

Figure 5.6. *Data processing flowchart.*

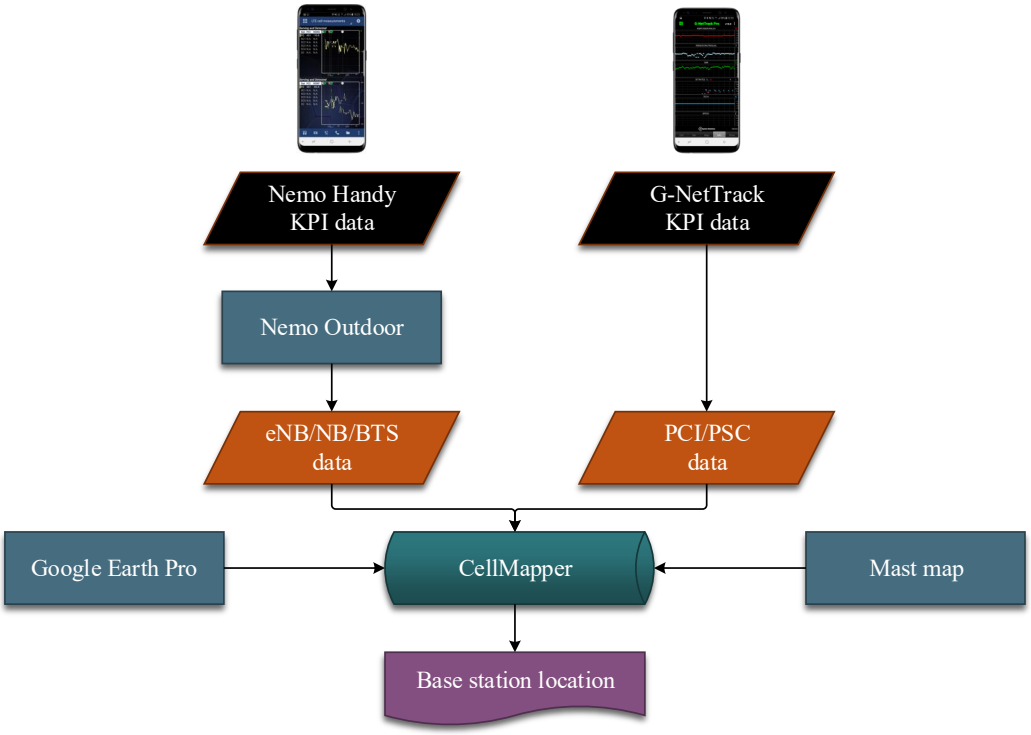

Figure 5.7. *Base station location process.*

6. MEASUREMENT RESULTS AND ANALYSIS

As per the goals of this thesis, the measurement results focus on three main attributes: signal strength, signal quality, and signal range. Some analysis is also done on handovers. For each measurement location, only a few figures have been chosen for further analysis. The complete results are available in appendix A. This chapter also compares the measurement results against known path loss models. Furthermore, a more detailed analysis about the overall results can be found in chapter 6.2.

6.1 Measurement results

Comparing the results between the different technologies is not that relevant, since they have different definitions for signal power and quality. Moreover, all the parameters effecting the results (base station locations, antenna configuration, propagation conditions, and network parameters) are different between the measurement sites. For every measurement location, the results of a few measurements are analyzed more carefully. Additionally, a single image depicts the base station ranges that the UE was connected to. For some sites, there is an additional image for base station connectivity at the ground level. These results are shown with a map service from the National Land Survey of Finland [44]. However, this comparison is not completely accurate, since the ground measurement have been obtained near the drone landing zone. Since the terrain was quite impassable on foot or with a car, it was not feasible to repeat the mobility routes on the ground level. This comparison still shows the effect of UE altitude to the possible signal range.

Furthermore, all of these results have been obtained in normal conditions, where the cellular network is operating without any disruptions. In electrical grid disturbance scenarios, the results might vary considerably. For example, if the nearby base stations are inoperable, the UE might connect to further base stations more easily. This is because the nearby base station signal would not interfere with the signals from other, more distant, base stations.

Table 6.1 depicts the color legends used in the figures. Blue represents drone altitude, red corresponds to signal strength, green means signal quality, and purple serves as handovers. For the sake of clarity, PCI, PSC, and BTS identifiers have been simplified, that is, their values have been replaced with natural numbers. There are no signal quality results for GSM measurements because the 2G quality measurements are not recorded by either of the drive test tools.

Table 6.1. *Measurement figure color legend.*

Color	Attribute
Blue	Drone altitude (m)
Red	Signal strength (dBm)
Green	Signal quality (dB)
Purple	Handovers

6.1.1 Pinsiö

KPI results

Figure 6.1 depicts the results of the Pinsiö 4G measurements at 150 m altitude. The autonomous mission start and stop times have been indicated with arrows. Usually, the mission begins when the drone has reached its mission altitude (either 50 m, 100 m, or 150 m) and ends shortly before the drone starts to descend. The first graph illustrates how the RSRP changes in relation to the drone altitude. At ground level, the RSRP is about -120 dBm, while at the flight route, at 150 m, the RSRP is about -80 dBm. This 40 dB difference in power means a 10000 times more powerful signal on a linear scale.

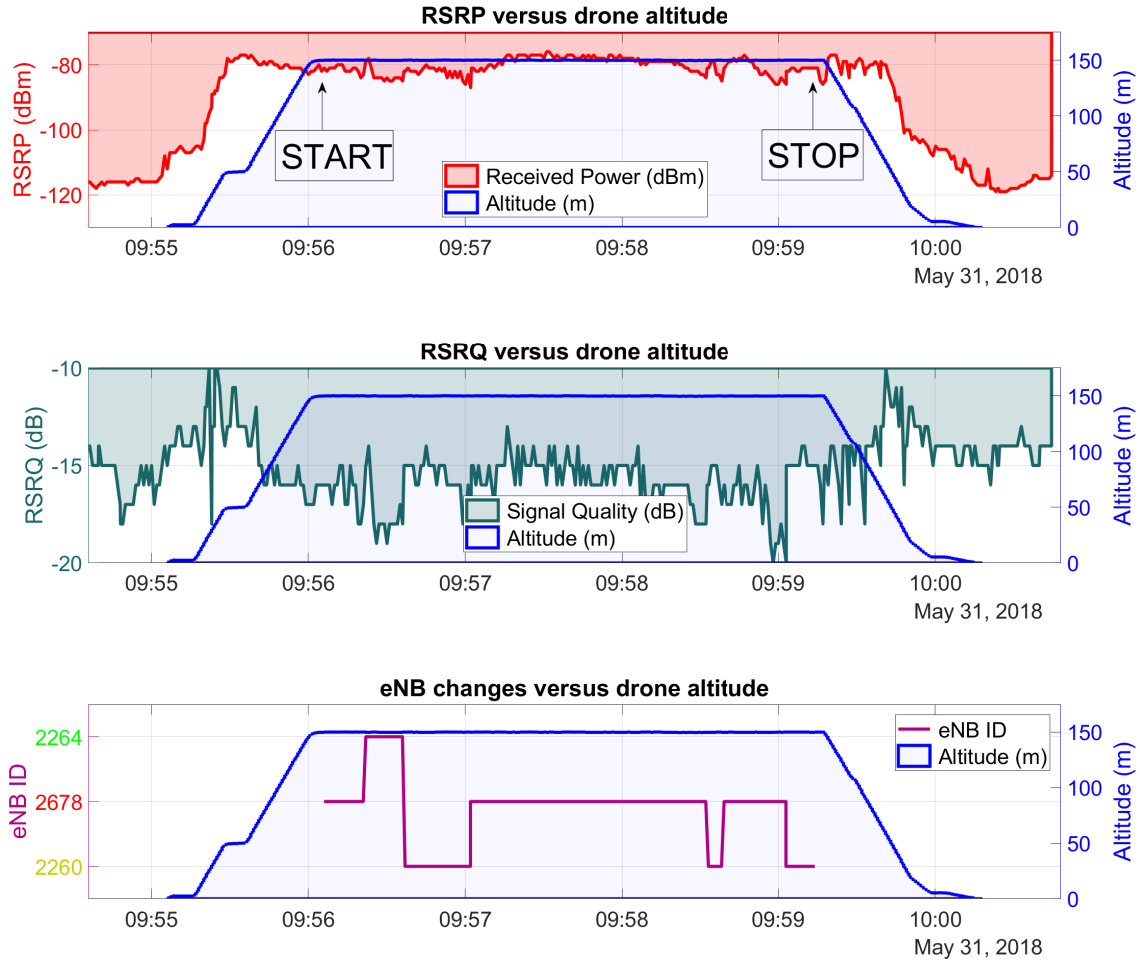

Figure 6.1. *Pinsiö 4G 150 m measurement.*

The middle graph shows RSRQ changes during the flight. Disregarding a few spikes when the drone is ascending and descending, the signal quality remains relatively constant throughout the measurement. The last graph displays PCI changes, that is, handovers, during the measurement. The UE changes between three cells during the mission.

Another way of examining the handovers is to look at a graph generated by G-NetTrack Pro. Figure 6.2 depicts the eNB IDs by color for all three altitudes. The majority of the time, the UE is connected to eNB 2678 (red), but on certain sections of the mobility route, the connection changes to eNB 2264 (green) or eNB 2260 (yellow). The corresponding handovers at 150 m altitude can be observed in figure 6.1.

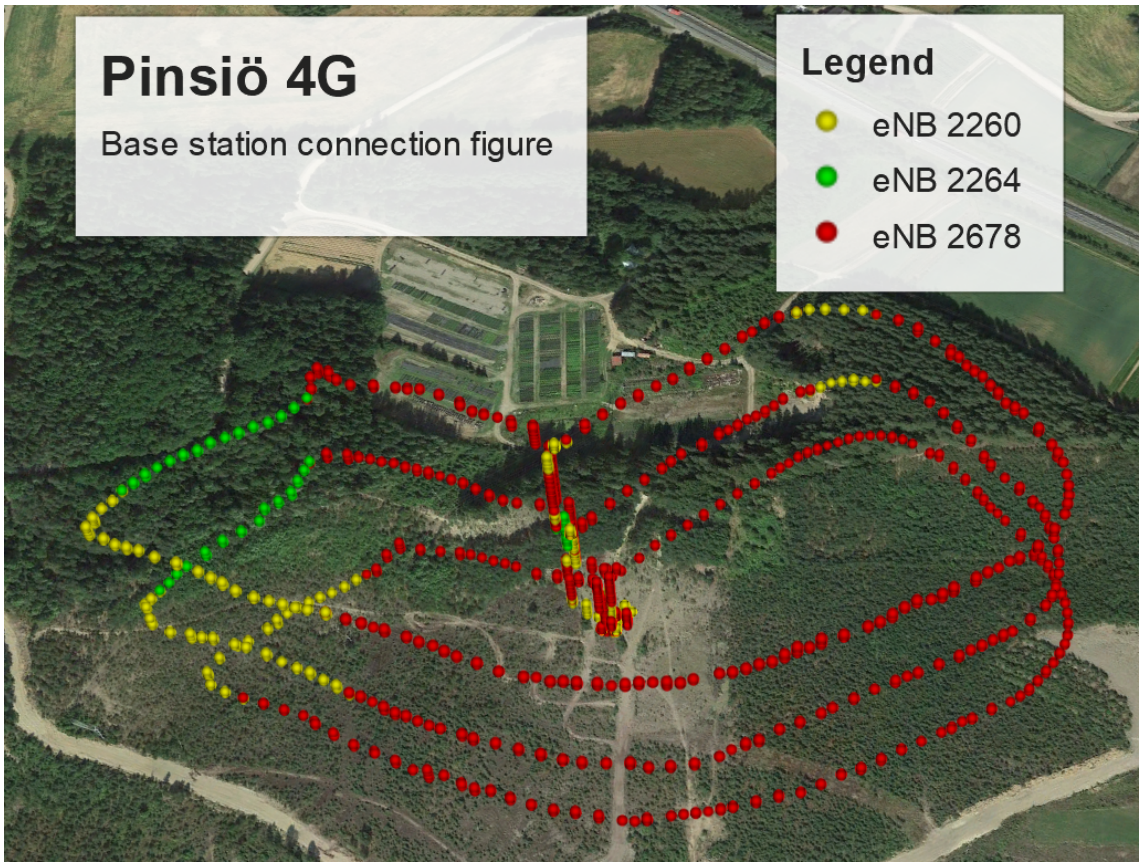

Figure 6.2. *Pinsiö 4G eNB connection graph. (Google Earth Pro)*

Figure 6.3 depicts the results of Pinsiö 3G measurements at 100 m altitude. The RSCP difference between the flight altitude of 100 m and ground level is about 20 dB, that is, 100 times on a linear scale. There are significant drops of received power around the 10:17 and the 10:18 time ticks. These correspond to the handovers at the same time. As the UE experiences a loss of RSCP, it initiates a handover procedure. The quality persists between -10 dB and -15 dB for most of the measurement.

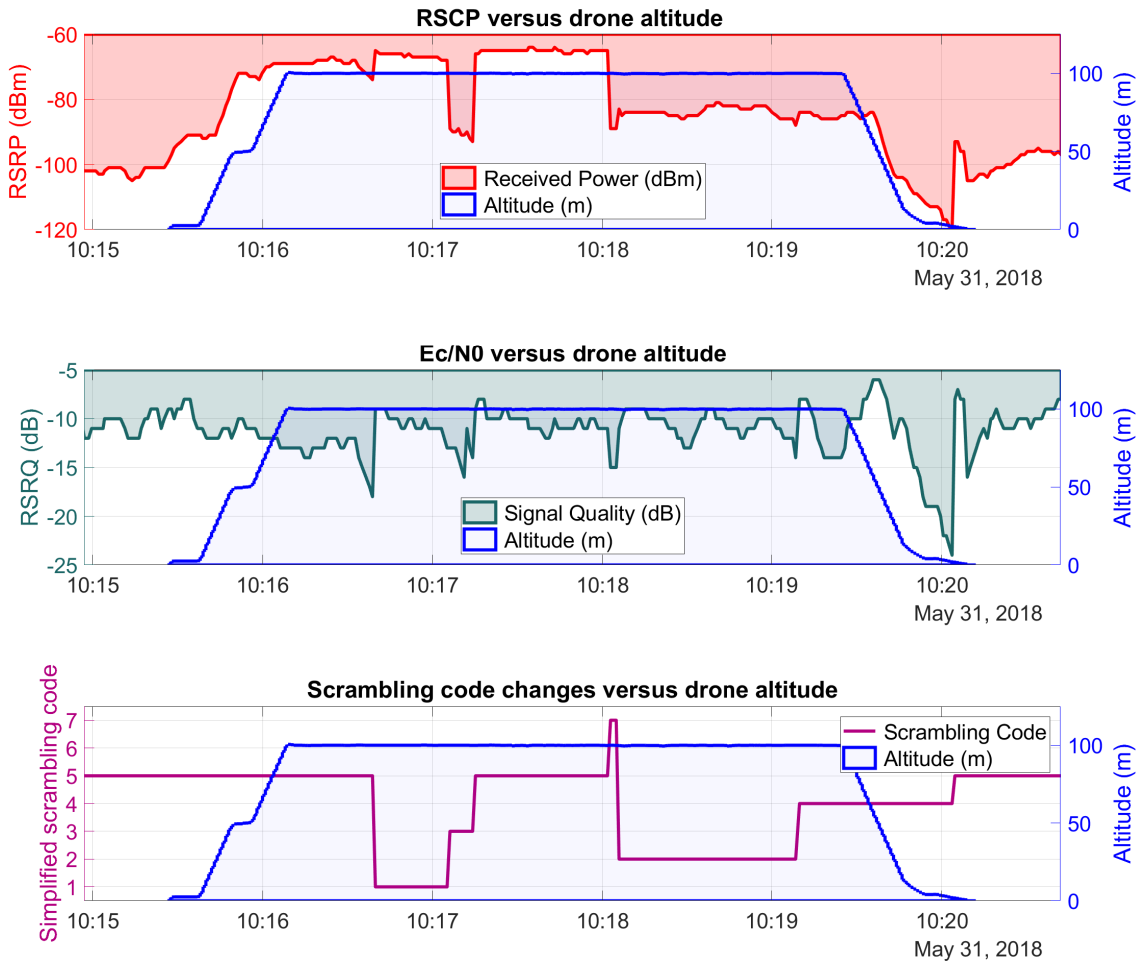

Figure 6.3. *Pinsiö 3G 100 m measurement.*

Base station locations at mission altitudes

Figure 6.4 displays the base stations that the UE was connected to at mission altitudes and their distance to the measurement site. The farthest 3G base station is about 33 km from the measurement site.

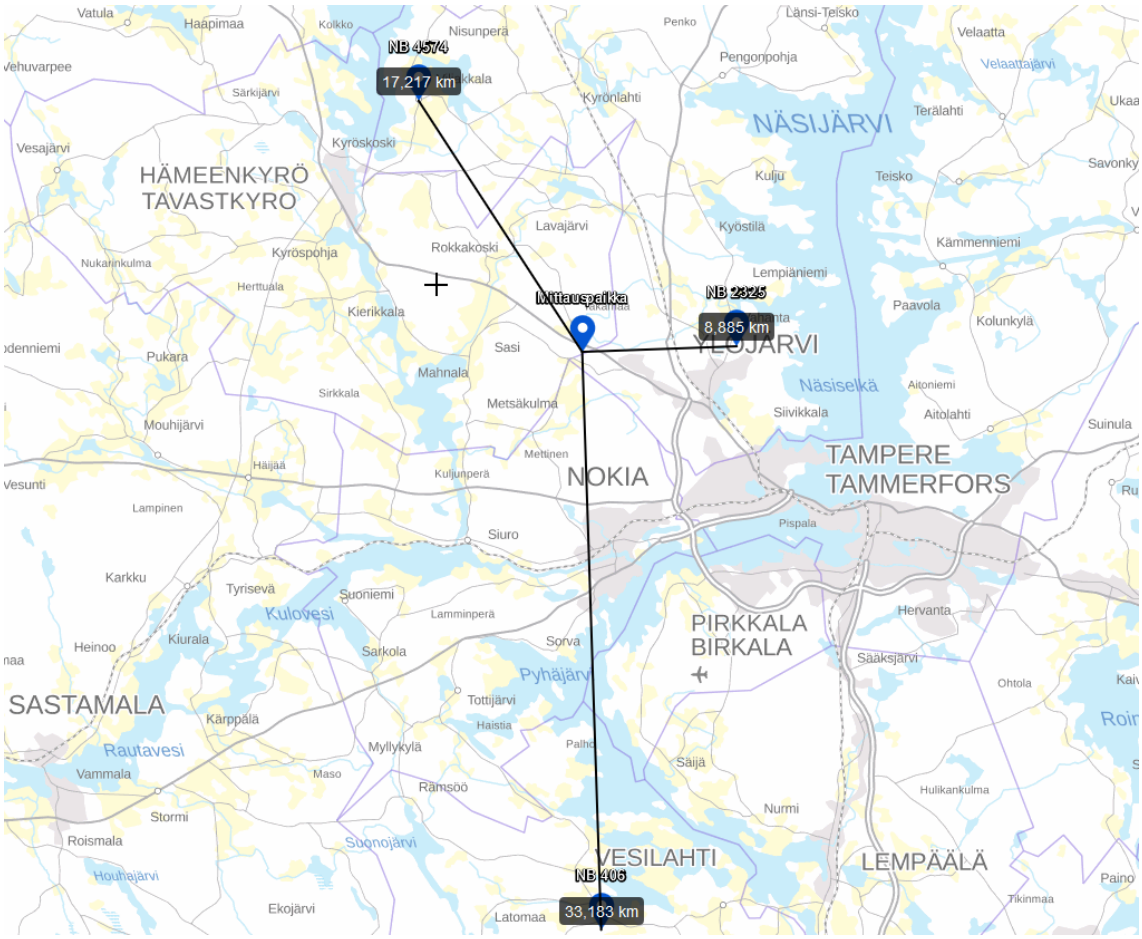

Figure 6.4. *Pinsiö 3G base station distances at flight altitudes. (Karttapaikka)*

6.1.2 Valkeakoski

KPI results

Figure 6.5a shows the results of Valkeakoski 4G measurements at 100 m altitude. The RSRP difference between ground level and 100 m is about 10–20 dB. RSRQ fluctuates according to altitude and handovers. The Valkeakoski 3G 100 m measurements are displayed in figure 6.5b. Received signal strength increases and signal quality decreases in accordance with the UE altitude.

Base station locations at mission altitudes

Figure 6.6 represents the 4G base station locations that the UE was connected to at mission altitudes. The furthermost base station is about 14 km from the measurement site.

Base station locations at the ground level

Figure 6.7 depicts the 4G base station location that the UE was connected to at the ground level. Since the nearby base station is so close to the measurement site, it overpowers any other signal from other base stations. Depending on the cellular network parameters, UEs

will only detect cells that are within a certain threshold of the serving cell received power. This comparison between ground level and flight altitude gives some indication about the increased signal range.

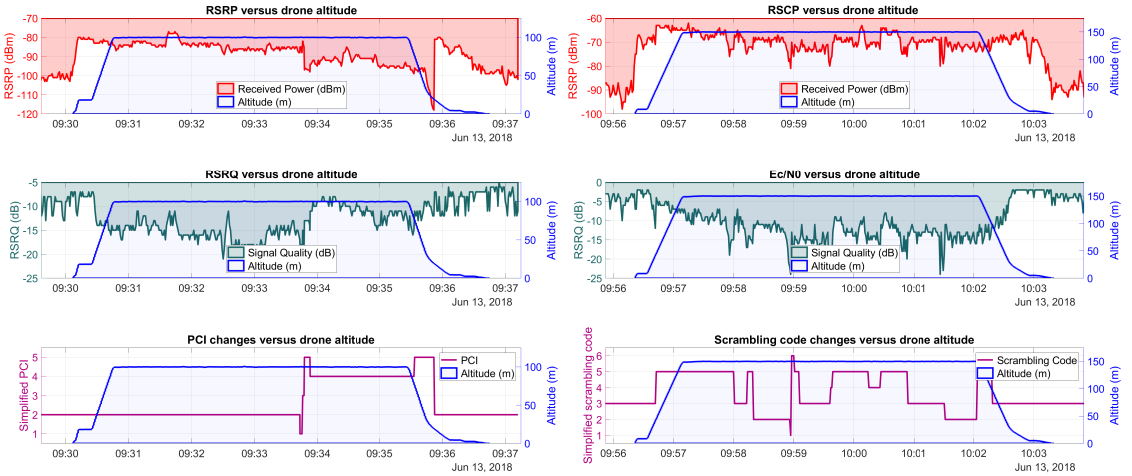

(a) *Valkeakoski 4G 100 m measurement.* ***(b)*** *Valkeakoski 3G 150 m measurement.*

Figure 6.5. *Valkeakoski measurements.*

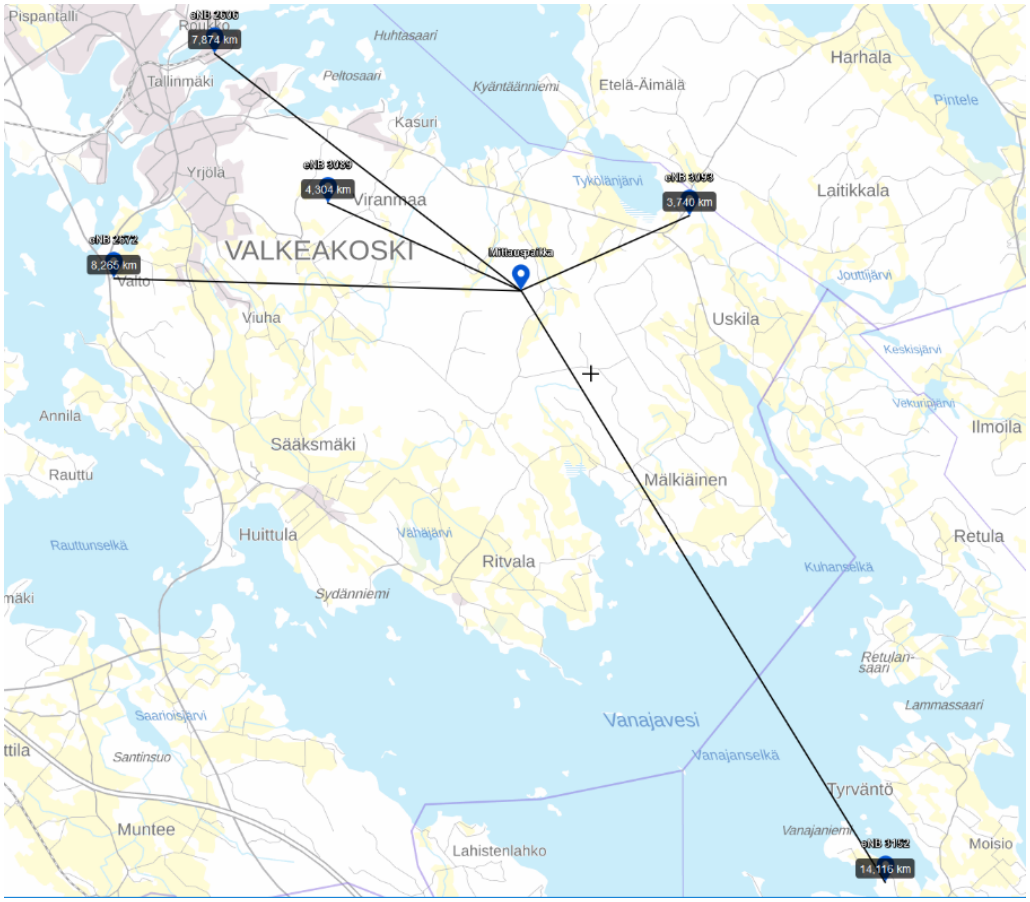

Figure 6.6. *Valkeakoski 4G base station distances at flight altitudes. (Karttapaikka)*

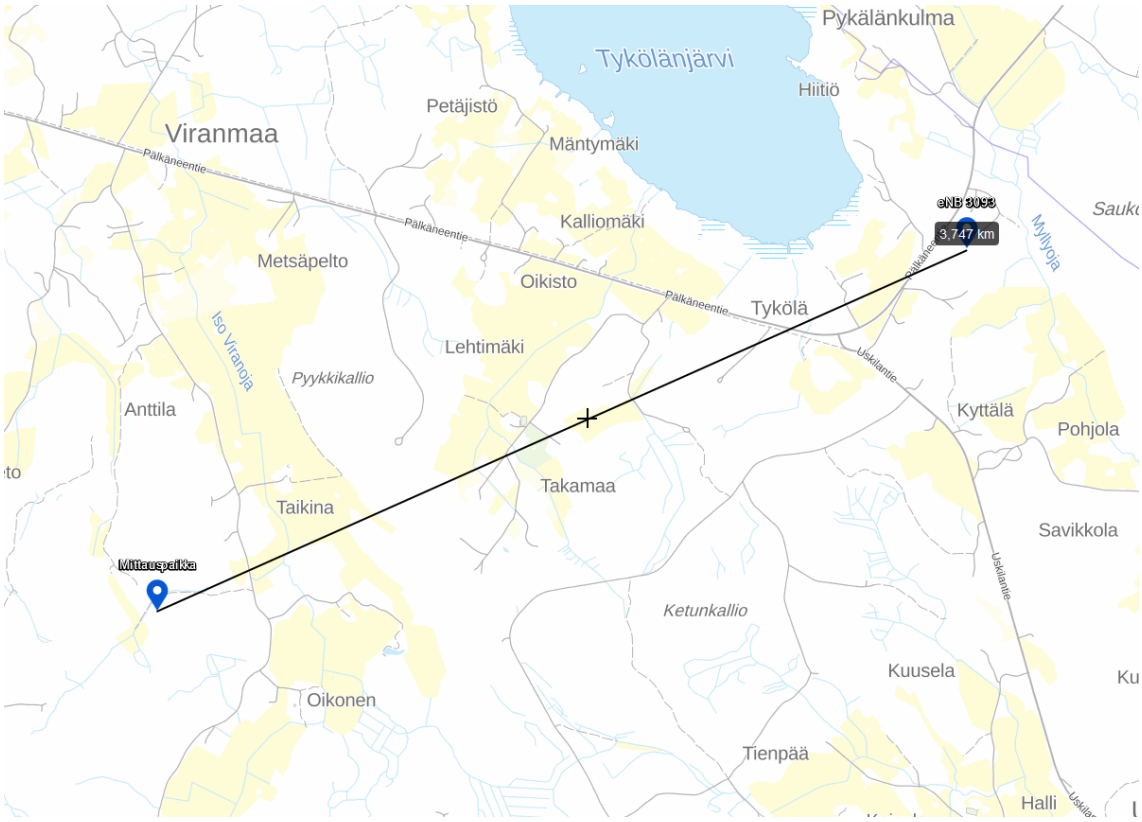

Figure 6.7. *Valkeakoski 4G base station distances at ground level. (Karttapaikka)*

6.1.3 Orivesi

KPI results

Figure 6.8a presents the results of Orivesi 3G measurements at 150 m. At 10:02, after several handovers, the signal power starts to drop drastically. A few seconds before 10:04, the connection returns to the previous level. This indicates that the drone mobility route can have a significant effect on the KPI parameters due to antenna patterns. Signal quality deteriorates only slightly as a result of the UE altitude increase. Conversely, the Orivesi 2G measurement at 50 m, as depicted in figure 6.8b, shows a very stable connection to a single base station. The downlink received power increases from -85 dBm to -55 dBm as the drone ascents to 50 m. Because the location of 2G base stations is scarcer than in 3G or 4G, the amount of base stations the UE connects to is usually very limited. In this measurement, there are no handovers whatsoever.

Base station locations at mission altitudes

Figure 6.9 displays the various UMTS base stations observed at flight altitudes. In addition to the close by Node Bs, the UE was connected to a base station over 11 km away from the measurement point.

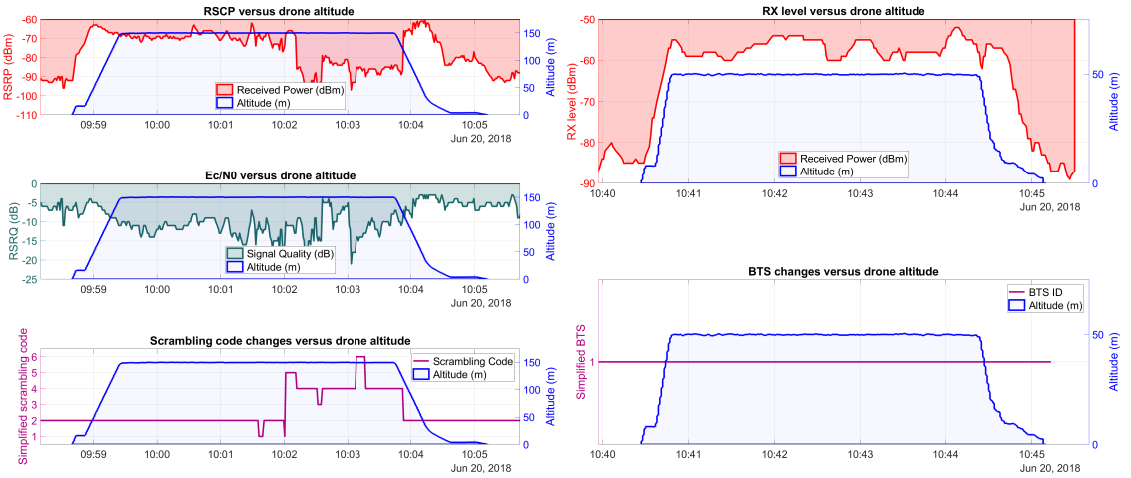

(a) *Orivesi 3G 150 m measurement.* ***(b)*** *Orivesi 2G 50 m measurement.*

Figure 6.8. *Orivesi measurements.*

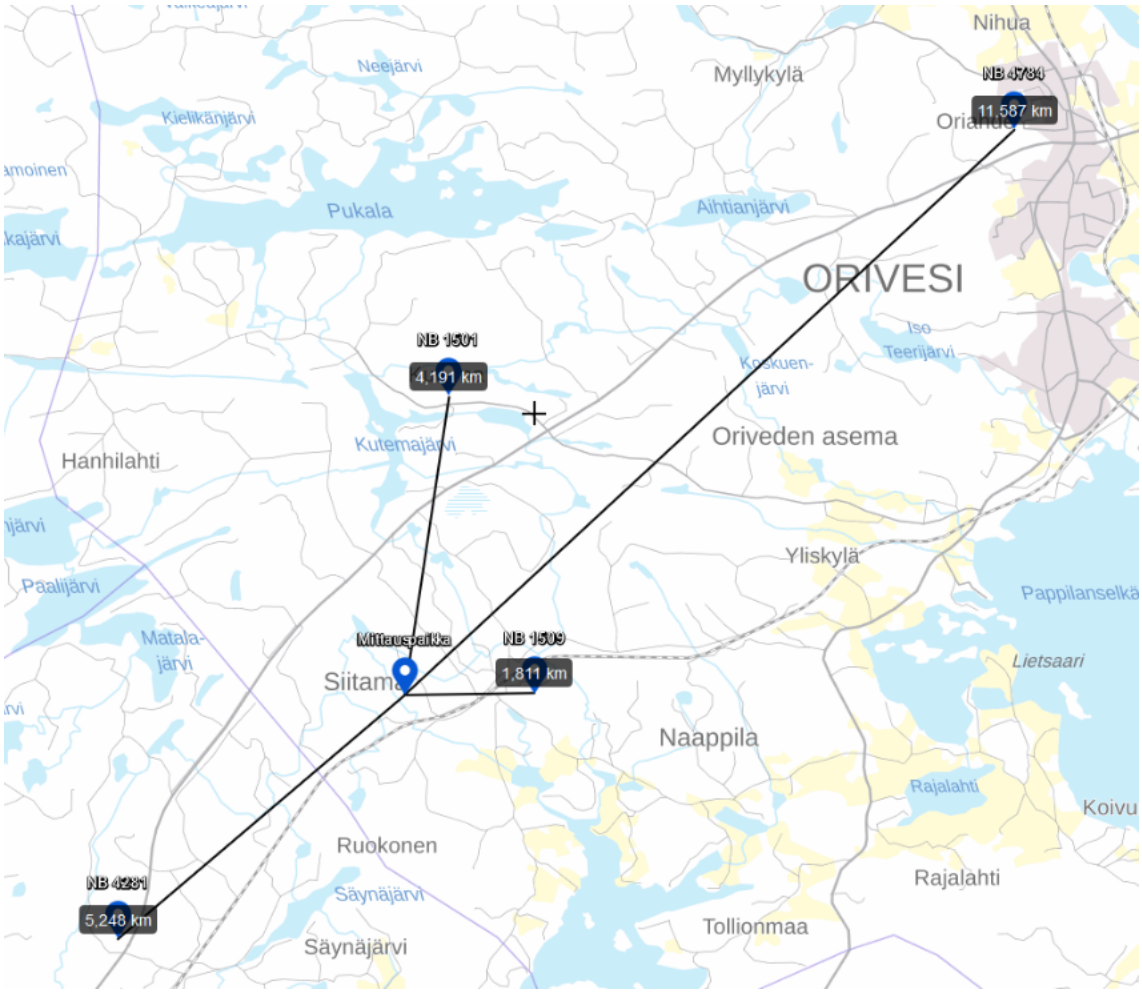

Figure 6.9. *Orivesi 3G base station distances at flight altitudes. (Karttapaikka)*

6.1.4 Nokia

KPI results

The Nokia 4G measurements, depicted in figure 6.10a, were notable. Instead of increased RSRP levels, like with the previous results, the signal power remained the same or even decreased with increased UE altitude. Despite a few handovers, the received power stayed poor during the flight. However, the signal quality behaved similarly to previous measurements, that is, it declined at flight altitudes. The increased number of visible base stations at mission altitudes causes more interference thus lowering the signal quality. The results were similar with the other elevation levels as well. The 3G results at 50 m, shown in figure 6.10b, followed a more familiar pattern. The RSCP increased about 20 dB at the flight altitude.

These results indicate that base station antenna direction and down tilt can have a drastic effect on the received power. Inevitably, there are going to be a few locations where an increased UE height will not have a significant impact on the signal power. However, based on our measurements, these situations are quite rare.

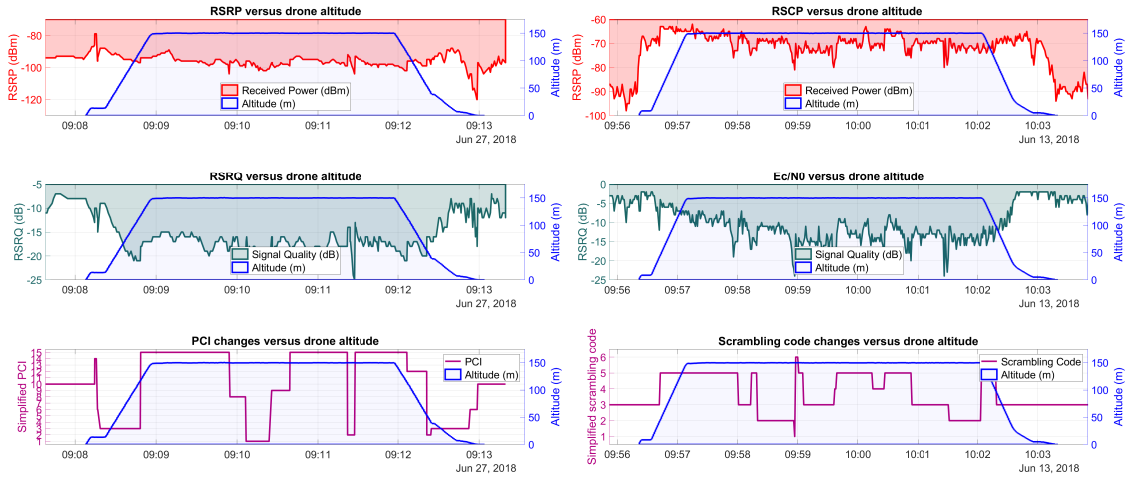

(a) *Nokia 4G 150 m measurement.* ***(b)*** *Nokia 3G 50 m measurement.*

Figure 6.10. *Nokia measurements.*

Base station locations at mission altitudes

Figure 6.11 marks the 3G base stations and their distances to the measurement site. Of note is the 39 km distance to the farthest base station.

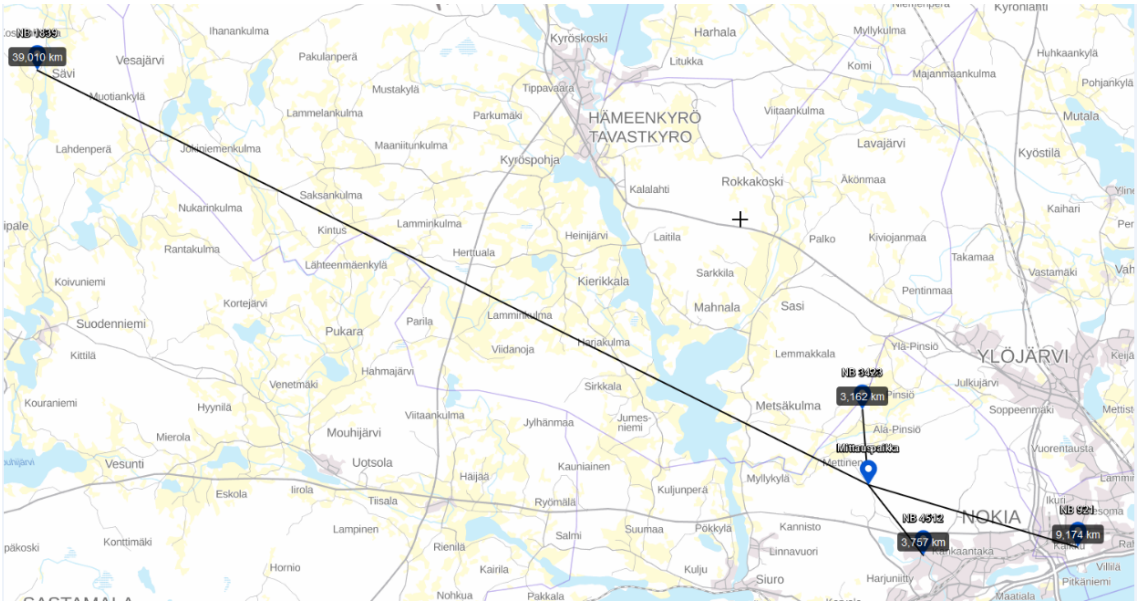

Figure 6.11. *Nokia 3G base station distances at flight altitudes. (Karttapaikka)*

6.1.5 Savonkylä

KPI results

As evidenced by figure 6.12, the Savonkylä 4G 100 measurement is somewhat similar to the Nokia case, where the RSRP does not change with altitude. However, in this case, there are sections of the drones mobility route, where the signal power raises about 30 dB. There are a lot of handovers during the flight.

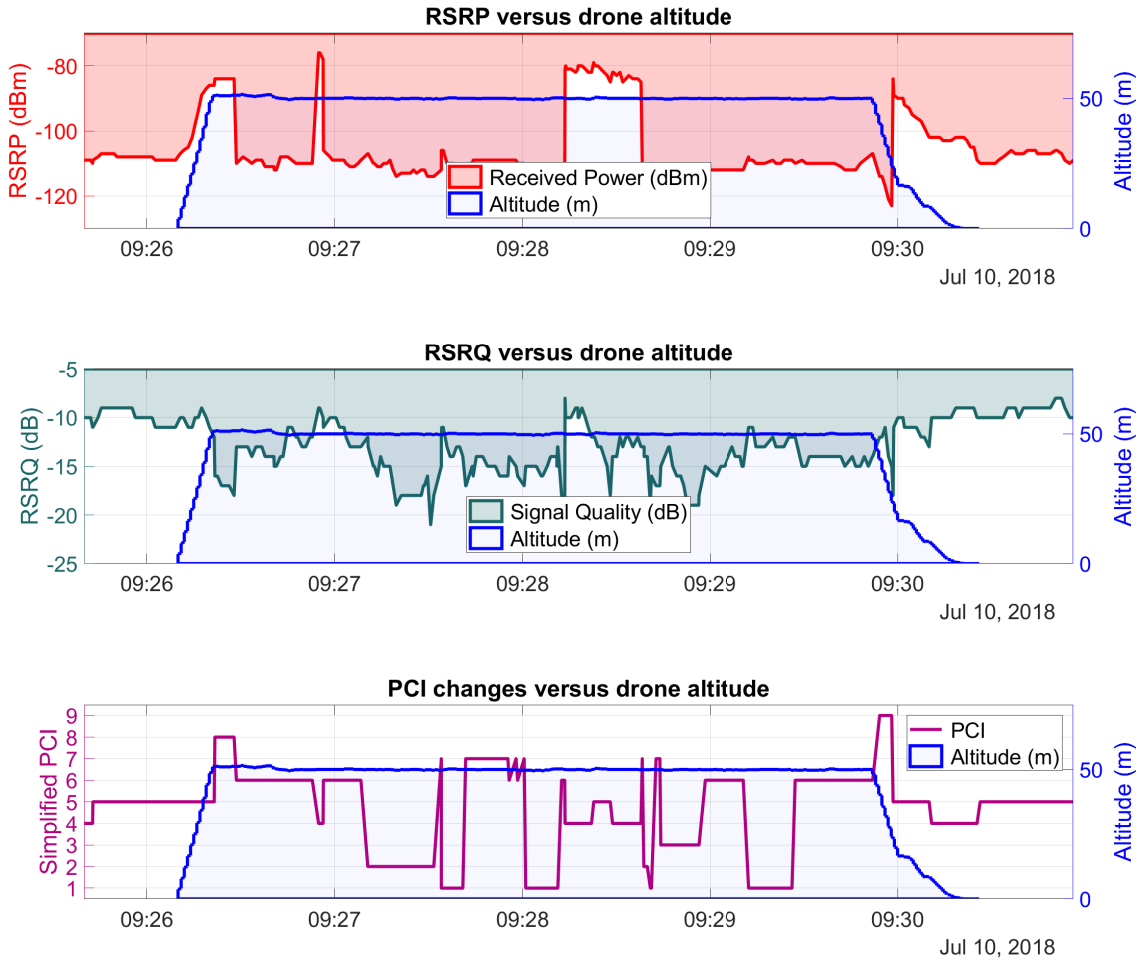

Figure 6.12. *Savonkylä 4G 50 m measurement.*

Base station locations at mission altitudes

The UE was connected to several LTE base stations at mission altitudes. Figure 6.13 shows only the three furthest ones.

Base station locations at the ground level

The base stations that the UE was connected at ground level are illustrated in figure 6.14. The maximum distance is 8 km on the ground while in the air, the distance to the farthest base station is 30 km. In this case, the signal range increase by over 20 km.

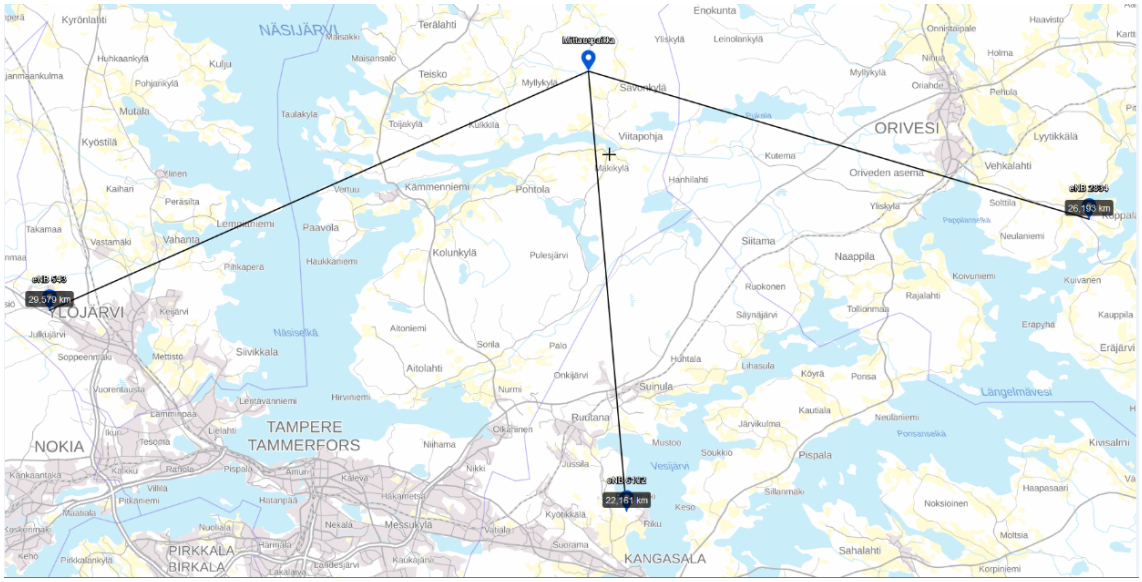

Figure 6.13. *Savonkylä 4G base station distances at flight altitudes. (Karttapaikka)*

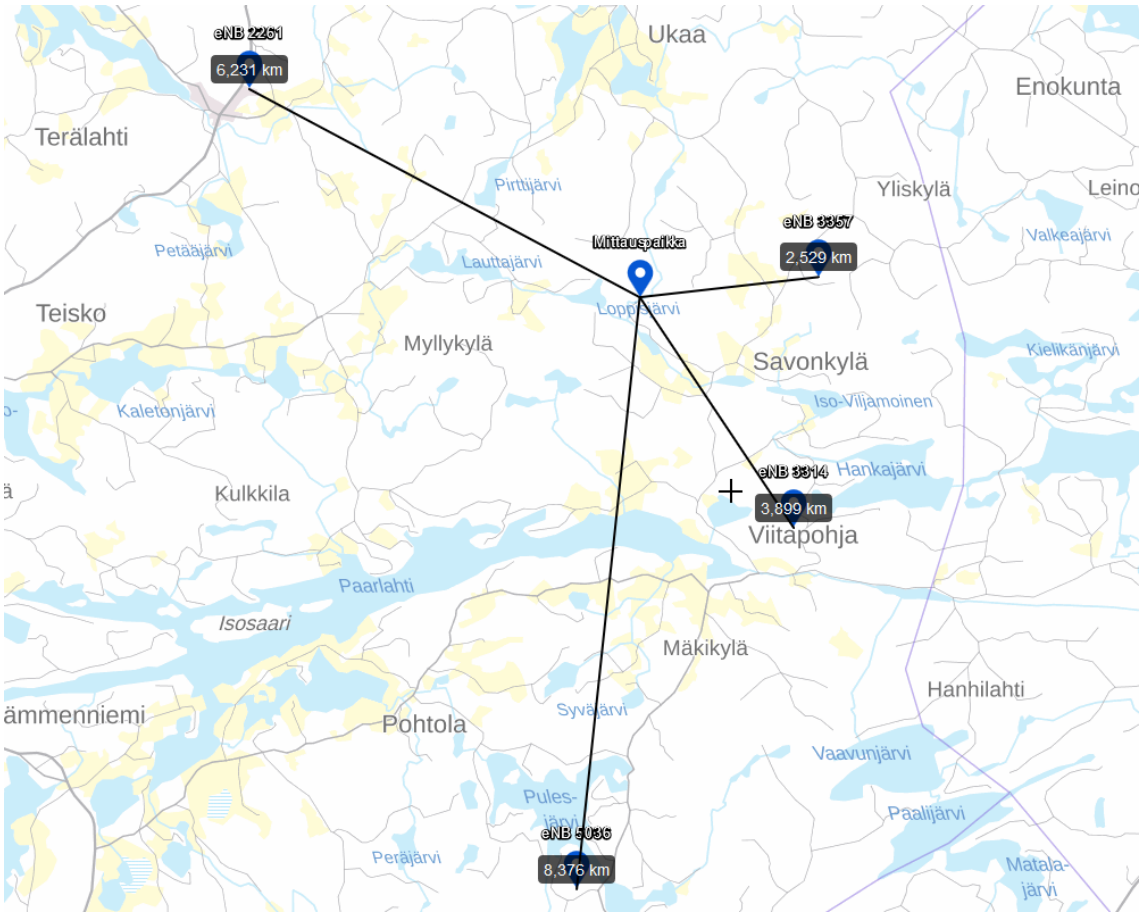

Figure 6.14. *Savonkylä 4G base station distances at ground level. (Karttapaikka)*

6.2 Analysis

The measurement results have been analyzed using four criteria. Signal power comparison examines the differences of downlink received power at ground level and at mission altitudes. Signal quality comparison does the same for the various quality KPIs. Signal range comparison uses the measured base station distances to draw conclusions of signal coverage. And finally, detected LTE neighbour cells analyses the effect of UE altitude on detected base stations. Additionally, this section addresses, how the measurements correlate with the theoretical path loss models.

6.2.1 Signal power comparison

The most significant factor to analyse is the received power because it correlates with signal range. The average results for all the altitudes are reported in tables 6.2, 6.3, and 6.4. The final column, *Air*, is the average of all the mission altitude results. Table 6.5 compares the average received power between the ground level and all the flight altitudes in decibels, that is, the *Ground* and *Air* columns, respectively. In table 6.5, a positive value means that the signal power is higher in the air and vice versa. These results have been obtained by combining the ground and the air measurement results into two separate vectors. These vectors were then converted to absolute power values, averaged, and then converted back to decibels. The comparison is then calculated as follows: Average received power comparison = Average signal power in the air - Average signal power on the ground.

Using the Pinsiö 4G result as an example, a 36 dB higher signal power in the air means a 4000 times higher power on a linear scale. To examine the effect this power increase has on signal range, free-space path loss can be used as a theoretical example. The distance part of the FSPL equation in 3.1 is:

$$20 \cdot \log_{10}(d_{\mathrm{km}}) \,.$$

Consequently, doubling the distance d_{km}, results into a 6 dB increase in the overall path loss. Furthermore, path loss can also be defined as:

$$PL = EIRP - RSRP \,.$$

which means that the higher the RSRP, the smaller the path loss. Essentially, a higher RSRP allows for a higher base station distance with the same path loss. As a result, a 36 dB higher RSRP allows for a theoretical $2^{(36/6)} = 2^6 = 64$ multiple to the signal range. A 64 times higher range is not realistic, but a more reasonable multiple of 10 to the signal range, however, is practical in a real world scenario. The base station distance results, discussed in chapter 6.2.3, are in accordance with these calculations.

As previously mentioned, these results can not be directly compared, since they have been collected with vastly different conditions. However, generally speaking, using an elevated UE can result into a 20–30 dB increase in signal strength. Moreover, almost across the board, the highest average received power is at the 50 m altitude. This is most likely as a result of the antenna heights and antenna down tilt at rural areas.

Table 6.2. *Average RSRP values at ground level and at mission altitudes (dBm).*

	RSRP (dBm)				
Location	**Ground**	**50 m**	**100 m**	**150 m**	**Air**
Pinsiö	-113.90	-76.23	-78.10	-79.8	-77.82
Valkeakoski	-101.10	-81.77	-84.55	-82.76	-82.88
Orivesi	-103.98	-74.40	-75.19	-77.43	-75.48
Nokia	-95.36	-99.48	-96.53	-96.17	-97.17
Savonkylä	-107.82	-87.98	-104.63	-85.14	-87.93

Table 6.3. *Average RSCP values at ground level and at mission altitudes (dBm).*

	RSCP (dBm)				
Location	**Ground**	**50 m**	**100 m**	**150 m**	**Air**
Pinsiö	-98.79	-65.83	-68.89	-71.77	-68.1
Valkeakoski	-85.97	-67.91	-68.37	-68.86	-68.36
Orivesi	-89.33	-60.96	-63.73	-69.67	-63.55
Nokia	-82.25	-63.86	-72.07	-73.17	-67.63
Savonkylä	-90.69	-61.39	-62.69	-63.99	-62.51

Table 6.4. *Average RX level values at ground level and at mission altitudes (dBm).*

	RX level (dBm)				
Location	**Ground**	**50 m**	**100 m**	**150 m**	**Air**
Pinsiö	-89.07	-52.62	-54.06	-54.39	-53.61
Valkeakoski	-83.41	-67.72	-68.13	-70.17	-68.52
Orivesi	-85.01	-56.56	-58.20	-62.07	-58.32
Nokia	-81.33	-64.01	-62.25	-64.12	-64.37
Savonkylä	-89.91	-58.29	-59.88	-62.36	-59.92

Table 6.5. *Average received power comparison between ground level and at mission altitudes (dB).*

Location	**LTE (dB)**	**UMTS (dB)**	**GSM (dB)**
Pinsiö	36.08	30.69	35.46
Valkeakoski	18.22	17.61	14.89
Orivesi	28.50	25.78	26.69
Nokia	-1.81	14.62	16.96
Savonkylä	19.89	28.18	29.99

6.2.2 Signal quality comparison

The average RSRQ and Ec/N0 values are listed in tables 6.6, and 6.7. Table 6.8 shows the RSRQ and Ec/N0 comparison between the ground and the air measurements. The results have been obtained with the same method as the previously presented signal power comparison. A negative value indicates that the signal quality was worse in the air than on the ground. The Pinsiö results are notable, since the quality got better in the air for both the 4G and the 3G cases. Generally speaking, the signal quality deteriorates a few decibels with the rise of altitude. This is caused by the increased interference from base stations that have a LOS connection to the UE in the sky. Furthermore, as with signal power, the highest aerial quality values are at an altitude of 50 m.

Table 6.6. *Average RSRQ values at ground level and at mission altitudes (dB).*

	RSRQ (dB)				
Location	**Ground**	**50 m**	**100 m**	**150 m**	**Air**
Pinsiö	-13.97	-9.92	-12.84	-15.79	-12.24
Valkeakoski	-8.51	-12.73	-13.17	-14.94	-13.50
Orivesi	-9.41	-9.91	-9.86	-11.45	-10.34
Nokia	-10.60	-12.15	-17.74	-17.26	-14.90
Savonkylä	-10.45	-13.38	-15.96	-15.26	-14.65

Table 6.7. *Average Ec/N0 values at ground level and at mission altitudes (dB).*

	Ec/N0 (dB)				
Location	**Ground**	**50 m**	**100 m**	**150 m**	**Air**
Pinsiö	-10.56	-8.07	-10.83	-11.35	-9.78
Valkeakoski	-3.76	-8.96	-10.97	-12.03	-10.47
Orivesi	-5.46	-5.03	-7.68	-10.40	-7.20
Nokia	-10.19	-10.11	-10.47	-12.61	-10.94
Savonkylä	-6.50	-6.25	-7.56	-9.91	-7.59

Table 6.8. *Average signal quality comparison between ground level and at mission altitudes (dB).*

Location	**LTE (dB)**	**UMTS (dB)**
Pinsiö	1.73	0.78
Valkeakoski	-3.16	-6.71
Orivesi	-0.93	-1.74
Nokia	-4.30	-0.75
Savonkylä	-4.20	-1.09

6.2.3 Signal range comparison

Ultimately, the purpose of this thesis was to study how the UE altitude effects signal range. Besides the range calculations due to increased signal strength, another way is to examine the base station distances that the UE was connected to. Table 6.9 depicts the distance to the furthest base station that the UE was connected to during the drone missions. In some cases, the signal of the nearby serving cell is too strong for the UE to connect to a farther away base station. However, for each location, at least one distance greatly exceeds the distances that are probable at the ground level.

Table 6.9. *Distance to the farthest base station (km).*

Location	LTE (km)	UMTS (km)	GSM (km)
Pinsiö	8.2	33.2	2.8
Valkeakoski	14.1	3.7	4.3
Orivesi	4.2	11.6	22.9
Nokia	11.2	39.0	7.7
Savonkylä	29.6	6.2	12.3

6.2.4 Detected neighbour cells

To further analyse the effect of UE height on detected base station cells, PCI, PSC, and RXlevelfullneighbor fields were examined for LTE, UMTS, and GSM, respectively. The number of detected cells have been separated into ground and air measurements. For LTE, the numbers shown in table 6.10 represent the number of detected unique PCI values. In the UMTS results, the numbers are the sum of unique scrambling codes in the active set and in the detected set. In the case of GSM, the results are the number of detected neighbor cells. The 2G mobile station (MS) maintains a list of neighbour cells. These cells and their received power measurements can be reported to the network.

Table 6.10. *The number of LTE, UMTS, and GSM detected cells at ground level and at mission altitudes.*

	LTE		UMTS		GSM	
Location	Ground	Air	Ground	Air	Ground	Air
Pinsiö	24	13	2	12	11	11
Valkeakoski	1	26	1	19	13	16
Orivesi	2	13	2	6	10	10
Nokia	44	46	4	8	12	14
Savonkylä	7	66	2	2	12	12

There are significant differences between the measurement sites in the amount of detected LTE cells. In Pinsiö, there are more detected PCIs on the ground than in the sky. In contrast to Pinsiö, the amount of detected cells at mission altitudes far exceed the results gathered from the ground level in Valkeakoski, Orivesi, and Savonkylä. Interestingly, the number of unique detected cells in Nokia is abundant for both ground and air measurements. The

UMTS numbers show a similar trend. At ground level there are only a few cells in the active or detected lists. However, as the altitude rises, the UE detects additional scrambling codes. There is very little difference between the ground and air results of detected GSM neighbour cells.

6.3 Comparison between path loss models and measurement results

Figure 6.15 and figure 6.16 shows a comparison between the path loss models and the measurement results at f_c = 800 MHz and f_c = 1800 MHz, respectively. Even though the modified Okumura-Hata and COST Hata models are not suitable for these conditions, they are shown here as a comparison. The path loss models have been calculated with the following parameters:

d_{2D} = 1–30 km,
h_{BS} = 60 m,
h_{UE} = 100 m,
f_c = 800 MHz or 1800 MHz, and
$G_{antenna}$ = 12 dBi.

The measurement results have been obtained from LTE measurements at a UE height of 100 m. These points were chosen from different sections of the drone mobility route and with different serving cell connections. The path loss values have been retrieved directly from the measurement results and they represent the median value of a few PL results. The UE calculates the path loss based on the base station transmit power (reported by the eNB) and its RSRP [18]. Therefore, it does not include the BS antenna gain. For this reason, a 12 dB gain has been added to the measured path loss values. The base station distances have been determined with the previously described method involving CellMapper.

For the most part, the measurement results seem to correspond with the path loss models. Most of the 800 MHz frequency band path loss results are within 10 dB of the 3GPP model. These differences can be explained by different base station antenna heights, antenna patterns, transmit powers, propagation conditions, and network parameters. These network configurations can also affect the measurement results. The results from base stations that are over 25 km from the measurement site, are slightly more inaccurate.

With the 1800 frequency band, the results show a similar trend. Most path loss measurements resemble the path loss models with an offset of about 10 dB or less. Even with the limited sample size and certain inaccuracies, these results show that the propagation conditions at these BS and UE heights resemble the 3GPP model with LOS conditions. Additionally, with these parameters, the 3GPP model almost parallels the FSPL model.

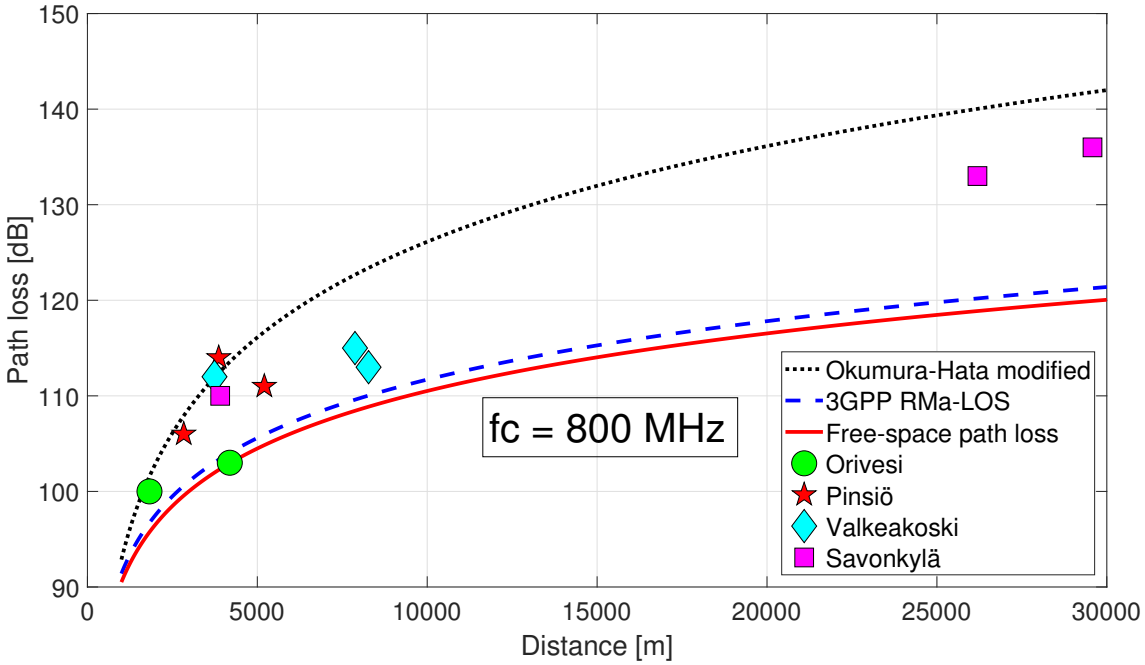

Figure 6.15. *Comparison between path loss models and LTE measurement results when $f_c = 800$ MHz.*

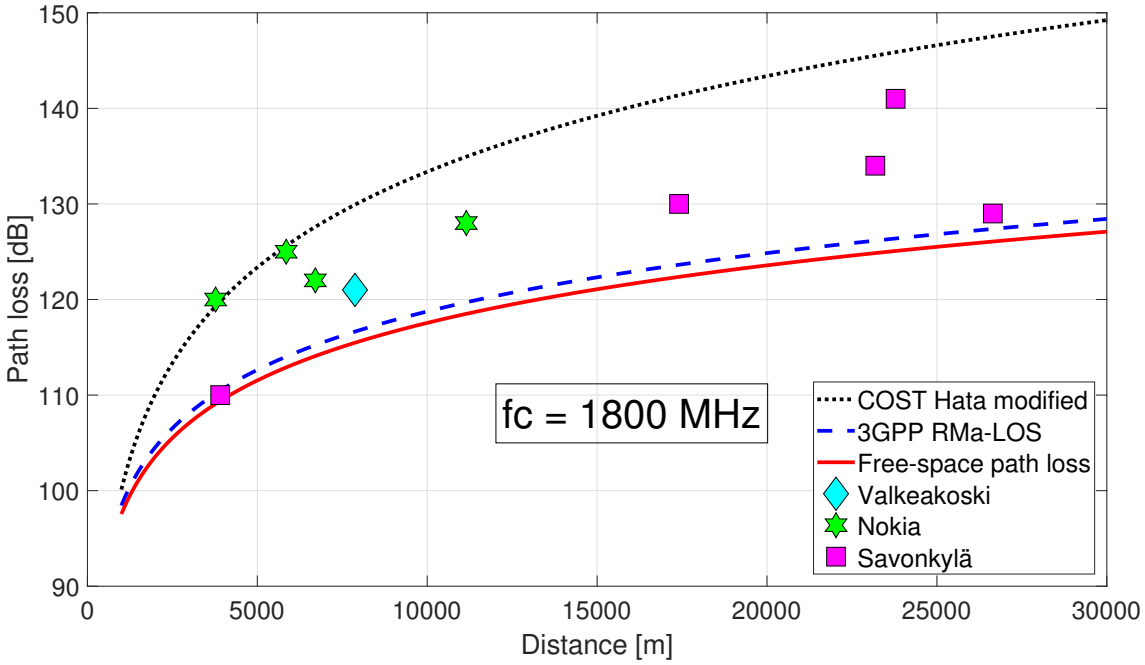

Figure 6.16. *Comparison between path loss models and LTE measurement results when $f_c = 1800$ MHz.*

7. CONCLUSION

This thesis examined the use of a drone in extending cellular coverage in electrical grid disturbance scenarios. The main focus was on cellular network measurements but to also study the feasibility of this ad hoc drone access point. The key research goal was to determine the effect of UE altitude on signal strength, signal quality, and signal range. To achieve this, several aerial measurements were conducted in five locations.

The results indicate that an increase in UE altitude does have a significant effect on cellular network KPI parameters. In the air, the downlink received signal strength increases 20–30 dB compared to the ground level. Consequently, this increase in power also affects signal range. The UE was able to establish a connection to base stations tens of kilometres away from the measurement site. This meant that the elevated UE was able to achieve a significantly higher signal range compared to the ground level. However, due to a high probability of LOS connections to several base stations, the UE suffers from increased interference, resulting in a worse signal quality of a few decibels. Additionally, the results suggest that the best connection in terms of signal strength and signal quality is at an altitude of 50 m. At this altitude, the UE is close to the BS antenna height but above the tree tops, resulting in the most optimal propagation conditions.

Nonetheless, these results have been obtained in normal conditions, where the cellular network is operating without any disruptions. In disturbance scenarios, with possible disruptions to cellular coverage, the results might be different. Moreover, the methodology concerning base station locations and their distances is somewhat inaccurate. Because the locations had to be determined using third party tools, there is a possibility of small errors. Nevertheless, the theory behind this solution is sound and the results are quite conclusive. Better propagation conditions result in a higher signal strength which in turn allows for a longer signal range.

Based on the results, the use of drones to enable a cellular connection during disturbance scenarios is a feasible option to explore for distribution system operators. Potentially, this solution would save time and money during disturbance scenario repair efforts. Due to the fact that the DSOs are already experimenting using drones in electrical grid repair and maintenance operations, this use case could strengthen the case of using drones as a helpful tool. However, the widespread utilisation of drones would require additional investments in equipment, training, and maintenance. Furthermore, disturbance scenarios happen so rarely that these expenses might not be cost-effective.

Further research on this subject should include using a dedicated access point mounted to the drone instead of a cell phone. Additionally, a network scanner would provide more

comprehensive results compared to a mobile phone. Another option is to use directional antennas to decrease interference to other UEs. Also, the effect of rain, wind, or low temperatures to the feasibility of this solution could be analysed. Overall, the whole concept of using a drone as a temporary way to provide connectivity or increase capacity could be explored in natural disasters situations, hiking, festivals, or concerts. However, since using a radio transmitter in the air and flying beyond visual line-of-sight drone missions require the appropriate permits, this might hinder the use of drones as access points for DSOs and other stakeholders.

Clearly, the future of drone connectivity is using cellular networks for drone command and control functionality. Considerable amount of research effort has been focused into LTE connectivity for drones. Either manually controlled or autonomous BVLOS use cases are crucial to many industries. Because cellular network connectivity is almost ubiquitous, there would be no range limitations as is the case with regular remote controllers. Additionally, the use of mobile networks would provide a secure wireless connectivity to increase the safety and reliability of drone operations.

REFERENCES

[1] 3GPP TR 36.777, “Enhanced LTE support for aerial vehicles”, Techn. rep., 2017. Available: ftp://www.3gpp.org/specs/archive/36_series/36.777/

[2] 3GPP TS 45.008, “GSM/EDGE Radio subsystem link control”, Techn. rep., 2018. Available: ftp://www.3gpp.org/specs/archive/45_series/45.008/

[3] Airdata UAV, 2018. Available (accessed on 7.10.2018): https://airdata.com/

[4] A. Al-Hourani, K. Gomez, Modeling cellular-to-UAV path-loss for suburban environments, IEEE Wireless Communications Letters, Vol. 7, Iss. 1, 2018, pp. 82–85.

[5] R. Amorim, P. Mogensen, T. Sorensen, I.Z. Kovács, J. Wigard, Pathloss measurements and modeling for UAVs connected to cellular networks, in: 2017 IEEE 85th Vehicular Technology Conference (VTC Spring), 2017, pp. 1–6.

[6] R. Amorim, H. Nguyen, P. Mogensen, I.Z. Kovács, J. Wigard, T.B. Sorensen, Radio channel modeling for UAV communication over cellular networks, IEEE Wireless Communications Letters, Vol. 6, Iss. 4, 2017, pp. 514–517.

[7] M.M. Azari, F. Rosas, A. Chiumento, K.C. Chen, S. Pollin, Coverage and power gain of aerial versus terrestrial base stations, in: Advances in Ubiquitous Networking 2, Springer, 2017, pp. 627–636.

[8] B.V.D. Bergh, A. Chiumento, S. Pollin, LTE in the sky: trading off propagation benefits with interference costs for aerial nodes, IEEE Communications Magazine, Vol. 54, Iss. 5, 2016, pp. 44–50.

[9] CellMapper, 2018. Available (accessed on 8.10.2018): https://www.cellmapper.net/

[10] E. Damosso, Digital mobile radio towards future generation systems: COST action 231, European Commission, 1999.

[11] M. Deruyck, J. Wyckmans, W. Joseph, L. Martens, Designing UAV-aided emergency networks for large-scale disaster scenarios, EURASIP Journal on Wireless Communications and Networking, Vol. 2018, Iss. 1, 2018, pp. 1–12.

[12] M. Deruyck, J. Wyckmans, L. Martens, W. Joseph, Emergency ad-hoc networks by using drone mounted base stations for a disaster scenario, in: International Conference on Wireless and Mobile Computing, Networking and Communications, 2016.

[13] A. Dhekne, M. Gowda, R.R. Choudhury, Extending cell tower coverage through drones, in: HotMobile 2017 - Proceedings of the 18th International Workshop on Mobile Computing Systems and Applications, 2017, pp. 7–12.

[14] DJI Inspire 2, 2018. Available (accessed on 28.9.2018): https://www.dji.com/inspire-2

[15] Droneinfo, 2018. Available (accessed on 6.10.2018): https://www.droneinfo.fi/en/no_drone_zones/download_droneinfo_app

[16] Elenia, 2018. Available (accessed on 6.9.2018): http://www.elenia.fi/yritys/about

[17] Elisa Oyj, 2018. Available (accessed on 4.10.2018): https://corporate.elisa.com/

[18] ETSI, TS 136 213 v14.3.0,“, LTE: Evolved Universal Terrestrial Radio Access (E-UTRA).

[19] ETSI, TS 144 018 v14.2.0 (Aug. 2017) Digital cellular telecommunications system (phase 2+), Mobile radio interface layer, Vol. 3.

[20] S. Euler, H.L. Maattanen, X. Lin, Z. Zou, M. Bergström, J. Sedin, Mobility support for cellular connected unmanned aerial vehicles: Performance and analysis, 2018.

[21] FICORA, 2018. Available (accessed on 4.10.2018): https://www.viestintavirasto.fi/en/index.html

[22] FICORA. Regulation on collective frequencies for licence-exempt radio transmitters and on their use, Jan 3, 2018. Available: https://www.viestintavirasto.fi/attachments/maaraykset/Regulation_15AM.pdf

[23] FICORA. Regulation on resilience of communications networks and services, Dec 17, 2014. Available: https://www.viestintavirasto.fi/attachments/maaraykset/Viestintavirasto54B2014M.pdf

[24] Fingrid, 2018. Available (accessed on 5.10.2018): https://fingrid.navici.com/

[25] Finnish Transport Safety Agency, 2018. Available (accessed on 6.10.2018): https://www.trafi.fi/en/aviation/unmanned_aviation

[26] Finnish Transport Safety Agency. Regulation OPS M1-32, 2018. Available (accessed on 6.10.2018): https://www.trafi.fi/filebank/a/1483970125/4a6ac53bf4b1cb434d7f85a15f36dde0/23661-OPS_M1-32_RPAS_2016_eng.pdf

[27] A. Fotouhi, M. Ding, M. Hassan, Flying drone base stations for macro hotspots, IEEE Access, Vol. 6, 2018, pp. 19530–19539.

[28] G-NetTrack Pro, 2018. Available (accessed on 3.10.2018): http://www.gyokovsolutions.com/G-NetTrackAndroid.html

[29] Goldman Sachs, Drones: Reporting for work. 25.04.2018. Available: http://www.goldmansachs.com/our-thinking/technology-driving-innovation/drones/

[30] Google Earth Pro, 2018. Available (accessed on 3.10.2018): https://www.google.com/earth/desktop/

[31] Google Maps, 2018. Available (accessed on 5.10.2018): https://www.google.com/maps/

[32] GSMA, Mobile-enabled unmanned aircraft, whitepaper, 2018. Available: https://www.gsma.com/iot/wp-content/uploads/2018/02/Mobile-Enabled-Unmanned-Aircraft-web.pdf

[33] M. Hata, Empirical formula for propagation loss in land mobile radio services, IEEE transactions on Vehicular Technology, Vol. 29, Iss. 3, 1980, pp. 317–325.

[34] H. Holma, A. Toskala, LTE for UMTS: Evolution to LTE-advanced, John Wiley & Sons, 2011.

[35] J. Laiho, A. Wacker, T. Novosad, Radio network planning and optimisation for UMTS, John Wiley & Sons, 2006.

[36] V. Leino, foreman, Infratek Oy Finland, 2018. Interview, 24.5.2018.

[37] J. Leskinen, Mast map, 2018. Available (accessed on 8.10.2018): https://mastot.jles.me/

[38] X. Lin, R. Wiren, S. Euler, A. Sadam, H.L. Maattanen, S.D. Muruganathan, S. Gao, Y.P.E. Wang, J. Kauppi, Z. Zou, V. Yajnanarayana, Mobile networks connected drones: Field trials, simulations, and design insights, 2018.

[39] X. Lin, V. Yajnanarayana, S.D. Muruganathan, S. Gao, H. Asplund, H.L. Maattanen, M.B. A, S. Euler, Y.P.E. Wang, The sky is not the limit: LTE for unmanned aerial vehicles, 2017.

[40] Litchi for DJI Mavic / Phantom / Inspire / Spark, 2018. Available (accessed on 3.10.2018): https://flylitchi.com/

[41] M. Mazur, A. Wiśniewski, J. McMillan, Clarity from above. PwC global report on the commercial applications of drone technology, PwC Polska, May, 2016.

[42] A.F. Molisch, Wireless communications, Vol. 34, John Wiley & Sons, 2011.

[43] S.D. Muruganathan, X. Lin, H.L. Maattanen, Z. Zou, W.A. Hapsari, S. Yasukawa, An overview of 3GPP release-15 study on enhanced LTE support for connected drones, 2018.

[44] National Land Survey of Finland, Karttapaikka, 2018. Available (accessed on 9.10.2018): https://asiointi.maanmittauslaitos.fi/karttapaikka/

[45] Nemo Handy Handheld Measurement Solution, 2018. Available (accessed on 30.9.2018): https://www.keysight.com/en/pd-2767485-pn-NTH00000A/nemo-handy?cc=FI&lc=fin

[46] H.C. Nguyen, R. Amorim, J. Wigard, I.Z. Kovács, P. Mogensen, Using LTE networks for UAV command and control link: A rural-area coverage analysis, in: 2017 IEEE 86th Vehicular Technology Conference (VTC-Fall), 2017, pp. 1–6.

[47] H.C. Nguyen, R. Amorim, J. Wigard, I.Z. Kovács, T.B. Sorensen, P.E. Mogensen, How to ensure reliable connectivity for aerial vehicles over cellular networks, IEEE Access, Vol. 6, ID: 1, 2018, pp. 12304–12317.

[48] No drone zones, 2018. Available (accessed on 4.10.2018): https://www.droneinfo.fi/en/no_drone_zones

[49] OpenCellID, 2018. Available (accessed on 9.10.2018): http://wiki.opencellid.org/wiki/FAQ#Long_cell_ID_vs._short_cell_ID

[50] P. Pisilä, Android-puhelimen firmware-etäpäivitys, Oulun ammattikorkeakoulu, 2014.

[51] M. Riikonen, project manager, Elite Group, 2018. Interview, 21.5.2018.

[52] L. Rytky, technician, Infratek Oy Finland, 2018. Interview, 21.5.2018.

[53] J. Säe, Aspects of Critical Communications in Disturbance Scenarios, Tampere University of Technology, Tampere University of Technology. Publication, Apr. 2017.

[54] L. Sundqvist, Cellular controlled drone experiment: Evaluation of network requirements, master's thesis, 2015. Available: http://urn.fi/URN:NBN:fi:aalto-201512165670

[55] Tampere-Pirkkala Airport Control Zone, 2018. Available (accessed on 4.10.2018): http://umap.openstreetmap.fr/en/map/ilmailukartta-droneharrastajalle_139199#11/61.4168/23.6546

[56] E. Teng, J.D. Falcao, B. Iannucci, Holes-in-the-sky: A field study on cellular-connected UAS, IEEE, pp. 1165–1174.

[57] TUT ProLab, 2018. Available (accessed on 2.10.2018): http://www.tut.fi/fi/yrityksille/palvelut-pk-yrityksille/tutlab-yhteisollinen-verstas/index.htm#Yrityksille

[58] International Telecommunication Union, Calculation of free-space attenuation, recommendation ITU-R pp.525-3, 2016. Available: https://www.itu.int/dms_pubrec/itu-r/rec/p/R-REC-P.525-3-201611-I!!PDF-E.pdf

[59] K. Welch, Evolving cellular technologies for safer drone operation, Qualcomm 5G White Paper and Presentations, Tech. Rep, 2016.

[60] V. Yajnanarayana, Y.P.E. Wang, S. Gao, S. Muruganathan, X. Lin, Interference mitigation methods for unmanned aerial vehicles served by cellular networks, arXiv preprint arXiv:1802.00223, 2018.

[61] G. Yang, X. Lin, Y. Li, H. Cui, M. Xu, D. Wu, H. Rydén, S.B. Redhwan, A telecom perspective on the internet of drones: From LTE-advanced to 5G, arXiv preprint arXiv:1803.11048, 2018.

APPENDIX A: FULL MEASUREMENT RESULTS

Pinsiö

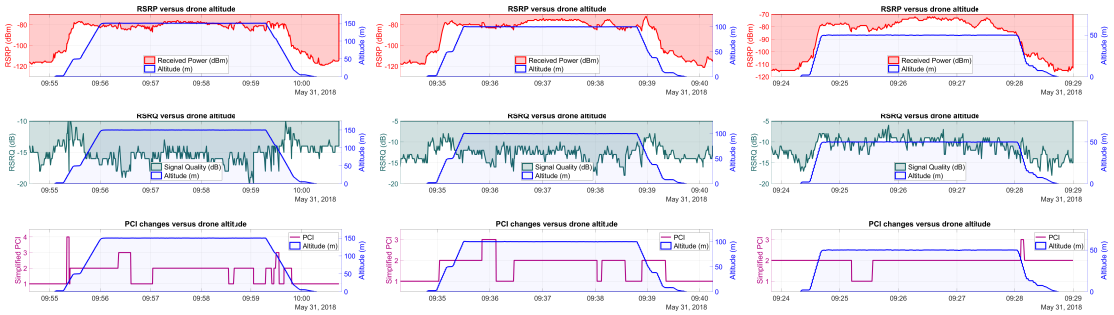

(a) 4G 150 m. *(b)* 4G 100 m. *(c)* 4G 50 m.

(d) 3G 150 m. *(e)* 3G 100 m. *(f)* 3G 50 m.

(g) 2G 150 m. *(h)* 2G 100 m. *(i)* 2G 50 m.

Pinsiö measurement results.

Valkeakoski

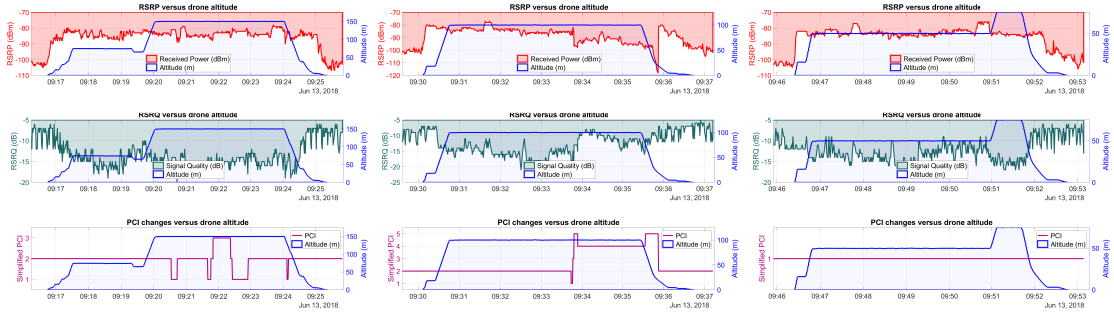

(a) *4G 150 m.* ***(b)*** *4G 100 m.* ***(c)*** *4G 50 m.*

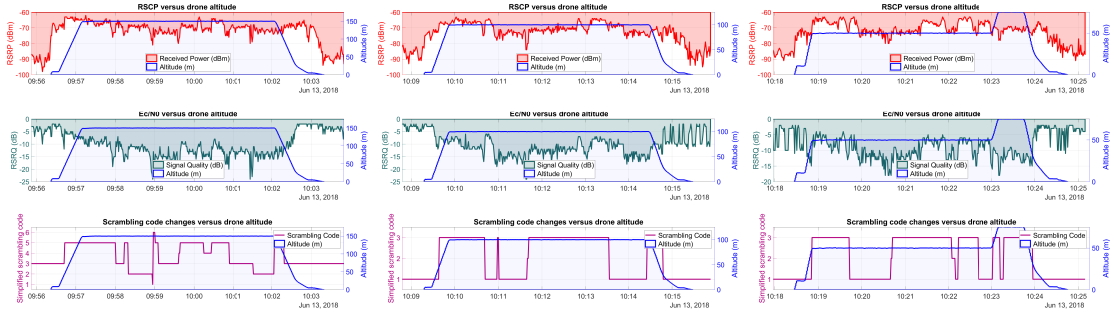

(d) *3G 150 m.* ***(e)*** *3G 100 m.* ***(f)*** *3G 50 m.*

(g) *2G 150 m.* ***(h)*** *2G 100 m.* ***(i)*** *2G 50 m.*

Valkeakoski measurement results.

Orivesi

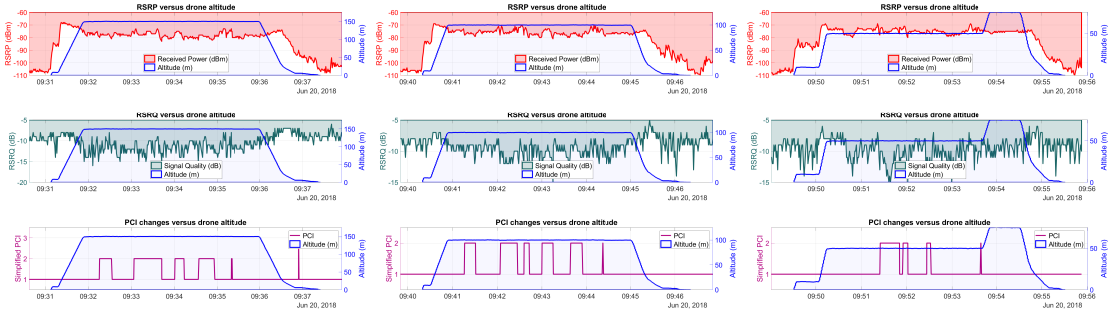

(a) *4G 150 m.* ***(b)*** *4G 100 m.* ***(c)*** *4G 50 m.*

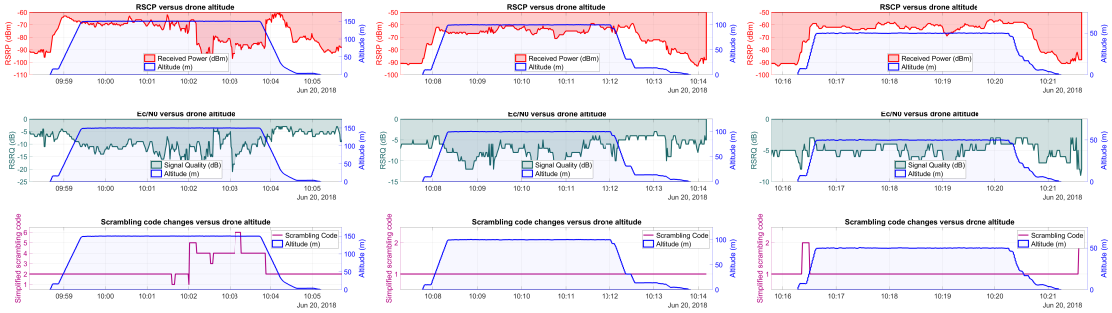

(d) *3G 150 m.* ***(e)*** *3G 100 m.* ***(f)*** *3G 50 m.*

(g) *2G 150 m.* ***(h)*** *2G 100 m.* ***(i)*** *2G 50 m.*

Orivesi measurement results.

Nokia

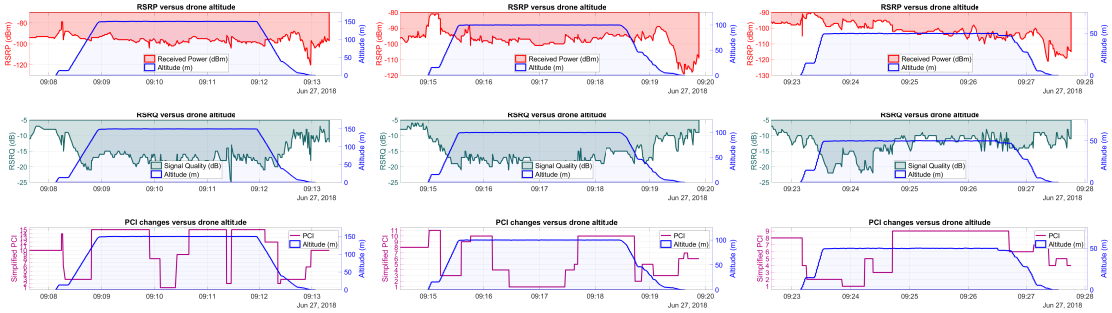

(a) *4G 150 m.*

(b) *4G 100 m.*

(c) *4G 50 m.*

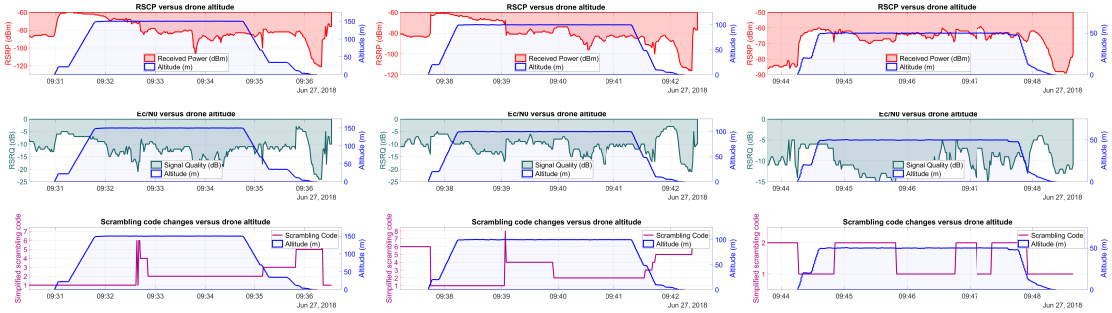

(d) *3G 150 m.*

(e) *3G 100 m.*

(f) *3G 50 m.*

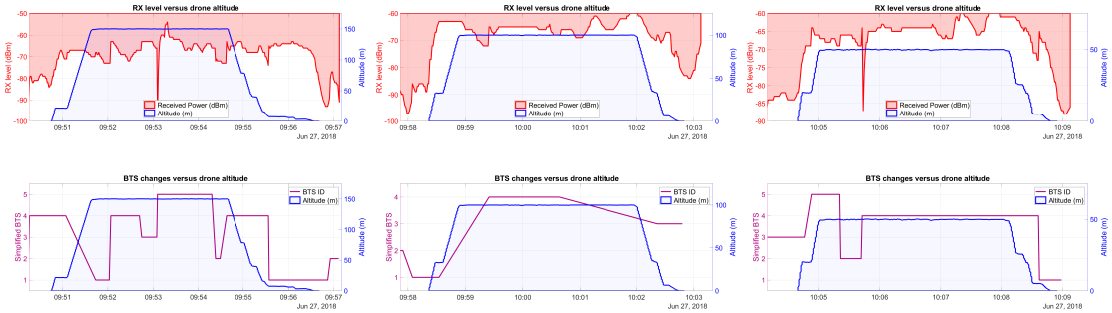

(g) *2G 150 m.*

(h) *2G 100 m.*

(i) *2G 50 m.*

Nokia measurement results.

Savonkylä

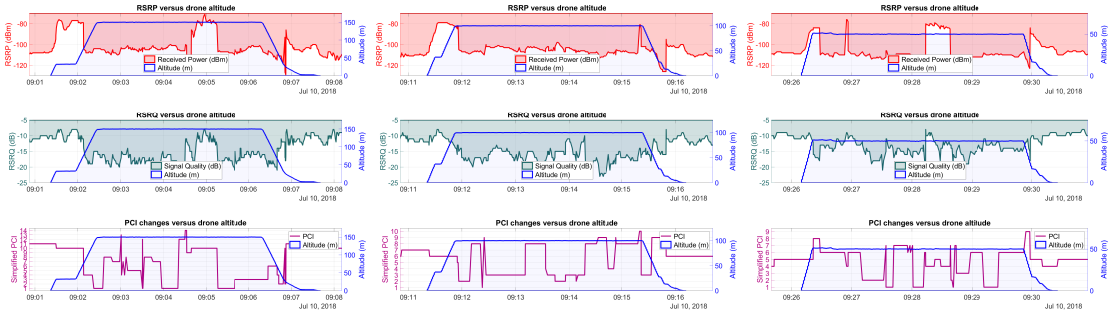

(a) *4G 150 m.*

(b) *4G 100 m.*

(c) *4G 50 m.*

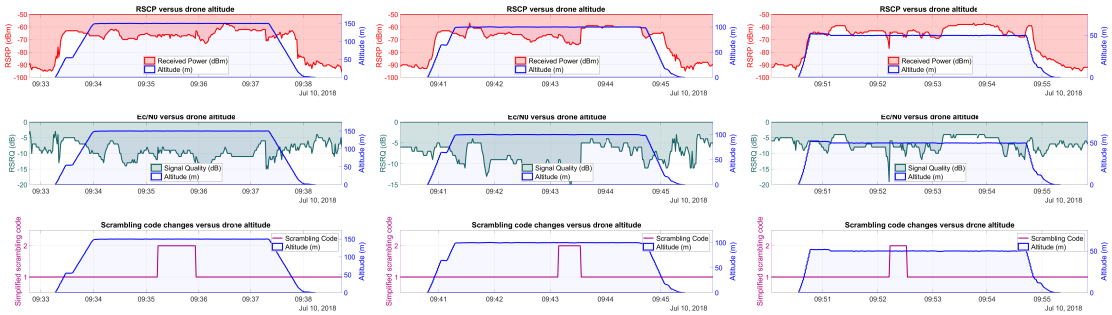

(d) *3G 150 m.*

(e) *3G 100 m.*

(f) *3G 50 m.*

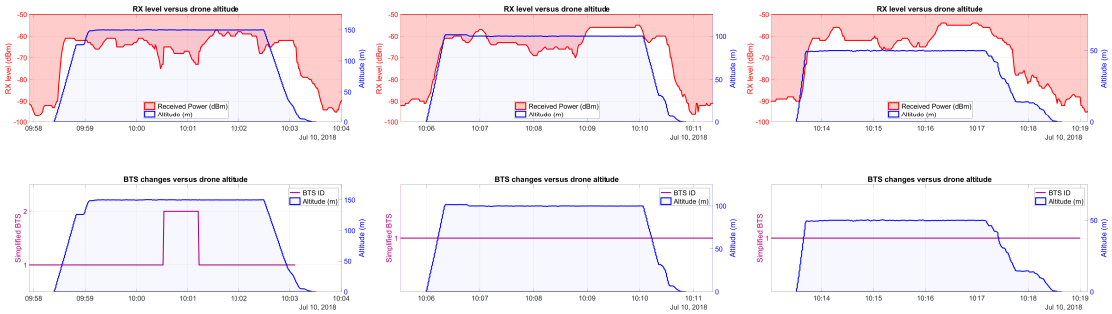

(g) *2G 150 m.*

(h) *2G 100 m.*

(i) *2G 50 m.*

Savonkylä measurement results.

APPENDIX B: DRONE SAFETY GUIDELINES AND PREFLIGHT CHECKLIST

Project DENCO Drone Safety Guidelines and Preflight Checklist[1]

Area and Environment

- Only fly in open areas.
- Check for cables, power lines, trees, bodies of water, or other obstacles near the flight route.
- Make sure there are no people or animals in the vicinity.
- Respect other people's privacy.
- Ensure that the pilot or spotter can maintain a visual line of sight to the drone at all times.
- Check for an alternative/emergency landing site in case the primary LZ gets compromised.
- Make sure the take-off/landing point has enough space to land the drone safely. Clear debris and vegetation if necessary.
- Only fly in good weather conditions:
  - Temperature > -10 degrees Celsius.
  - Wind speed < 10 m/s.
  - Clear visibility.
  - Avoid rain, snow, and fog.
- Avoid No-Fly Zones and restricted areas.
- Obey maximum flight altitude limits: 50 m near airports, otherwise 150 m.
- Always use visibility vests and a landing pad.

Drone, Remote Controller, and Flight Software

- Make a visual inspection of the drone before flight:
  - Check for loose screws, wiring, or connections.
  - Check that the propeller mounts and the propellers are free of damage.
  - Make sure the phone, camera, and batteries are properly seated and secured.
- Make sure that the flight app connects to the drone (restart if necessary).
- Ensure that both the drone and the flight app give the "Ready to Go (GPS)" signal with green indicators.

[1] Adapted from https://air-vid.com/uav-safety-checklist/ and DJI Inspire 2 user manual

- Calibrate the compass, camera, or IMU if necessary.
- Make sure all the firmware is up-to-date.
- Only use one flight app at a time.
- Check that all the drone, camera and Litchi settings are correct.
- Make sure there is enough battery power in all the components before taking off.
- Make sure the drone has all the necessary security settings turned on.
- Try to avoid frequency conflicts between the RC and the video transmission.
- Always turn off the drone before detaching the phone.

Mission Plan and Contingencies

- Plan all missions beforehand and check their feasibility with Google Earth or Virtual Litchi Mission.
- Before executing a mission, fly a shorter test mission.
- Check that there are no new obstacles in the flight path that were not visible in the planning stage.
- Always start automated missions while in the air.
- Assess the minimum safe altitude of the planned route if there are unforeseen obstacles.
- Try to execute the missions in a way that the drone will have more than 20% battery after completing the last mission with a pair of batteries.
- Remember to account for the time (and battery life) flying to the first waypoint and flying home from the last waypoint.
- Set appropriate cruising speed, maximum speed, RTH altitude and maximum altitude especially if flying in an area restricted to 50 m.
- If necessary, make adjustments to the missions at site.
- Things that affect flight time: weight of the drone, wind speed, temperature, and flight altitude.
- Litchi initiates a RTH at 20% battery (can be cancelled) and tries to land at the current spot at 10% battery (can still be controlled).

In-flight

- Make a Droneinfo announcement before taking off.
- Always keep your fingers on the RC.
- Never let the drone out of your sight.
- Keep the drone at a safe operating distance from people, trees, power lines, and buildings.
- In the case of an emergency, system failure, or degraded performance:
  - Immediately, try to find a safe place to land.
  - Try to regain manual control of the drone or initiate Return to Home (RTH) if necessary.
  - In the case of an automated mission, pause the mission with the pause button on the RC, or stop the mission by changing the flight mode from P to S.

  - Usually, the safest direction to dodge an object is to fly straight up.
  - Whenever anyone (pilot or spotter) notices a problem, that person should call it out with "STOP", "SEIS", or something of that sort to alert the others.
- If it's apparent that the batteries will go below 20% before the mission is complete, abort the mission by taking manual control and land the drone.

Technical details

- Inspire 2 operating temperature: -20° to 40° C.
- IPad Mini operating temperature: 0° C.
- Inspire 2 max take-off Weight: 4000g.
- Max wind speed resistance: 10 m/s.

Troubleshooting

- Change Gimbal to Free Mode (Arrow pointing northeast).
- Check that Main Controller settings > Advanced Settings > Sensitivity > Gimbal Yaw Smoothness is set to 0-30.
- In case of connectivity issues, restart everything in this order: RC, drone, flight app.
- If the RC keeps beeping (and blinking a red light), try calibrating the RC in the DJI Go 4 app.
- If the flight app has crashed or frozen, try the following:
  1. Disconnect the USB cable.
  2. Force close the app.
  3. Reconnect the USB cable.
  4. Run the app.
  5. (Turn the remote off and on).

Preflight checklist

- Droneinfo flight announcement.
- Insert the batteries to the drone (remove pin covers).
- Press the power button 5 times to enter Landing Mode.
- Power off drone.
- Attach the S8 mount.
- Mount the S8 (the lock faces the camera).
- Mount the camera (remove the cap from the camera and the drone, press the detach button, align white and red, rotate red to red to lock.
- Attach propellers (align red to red, insert propeller, push and turn until locked).
  - Check that all the propellers are firmly attached.
- Connect the iPad to the RC.
- Adjust the RC antenna angle (2,4GHz: 60 degrees, 5,8GHz: 90 degrees).
- Power the RC.

- Power the drone.
- Launch DJI Go 4/Litchi App.
  - (Perform compass calibration (click status bar, green light indicates success)).
  - (Perform IMU calibration (Main Controller Settings - Advanced Settings - Sensors)).
  - (Auto Gimbal calibration (General setting - Gimbal settings)).
- Check that everything is good to go:
  - DJI GO 4 App/Litchi: Ready to Go (GPS).
  - Drone: Slow green flashing = P-mode with GPS.

APPENDIX C: INTERVIEW SCRIPT

1. State your name, title, and company name please?
2. How does your company utilise drones in electrical grid repair or inspection operations?
3. A tree has fallen over an overhead power line. How does the repair process proceed from the drone use overview?
4. Are drones used to assess the damage in addition to locating the repair point?
5. How are the photographs that the drone takes utilised?
6. Are the photos just for the use of the repair crew or are they sent to the control center for analysis?
7. How many people belong to the drone repair crew?
8. How long does an average repair job take?
9. What kind of drone model are you using?
10. Does the repair workers require a constant connection to the control center?
11. Have you experienced situations, where the cellular network base stations are inoperable and the repair workers have to find a working connection by car?
12. Have there been any attempts to solve this problem?
13. This project examines using a drone as a mobile access point to enable a mobile connection from the repair site. Do you see any problems with this solution?
14. Have the repair workers got any drone training?
15. Are there any plans for training in the future?
16. Do the repair crew have any preconceptions towards drones?
17. Elenia has issued an incentive for the use of drones in electrical grid maintenance work. How effective has this program been?
18. Are there any restrictions that prevent the use of drones in certain conditions?
19. Is the drone's limited flight time an issue?
20. Do the cars have a way to charge the drone batteries?
21. What is the minimum distance between the drone and the power line?
22. Do you fly over the power line or next to it?
23. Does the existing legislation concerning BVLOS flights restrict drone operations?
24. Have you tested autonomous drone flights?
25. What is the biggest obstacle against a wide spread use of drones?
26. How do you see the usefulness of drones in electrical grid repair work? Are they already an indispensable tool?